Introduction to element based computing --- finite volume and finite element methods. Mesh generation

Joanna Szmelter
Loughborough University, UK

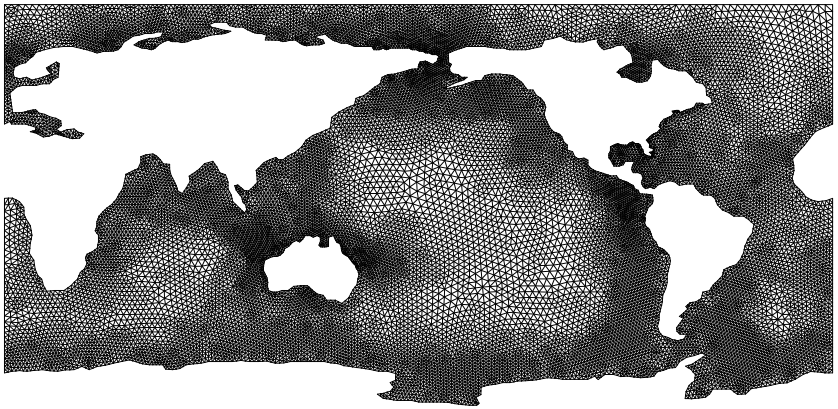

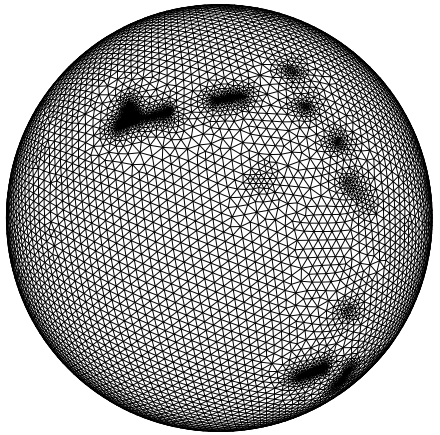

Traditional Discretisation Methods

- Finite Difference
- Finite Element
- Finite Volume

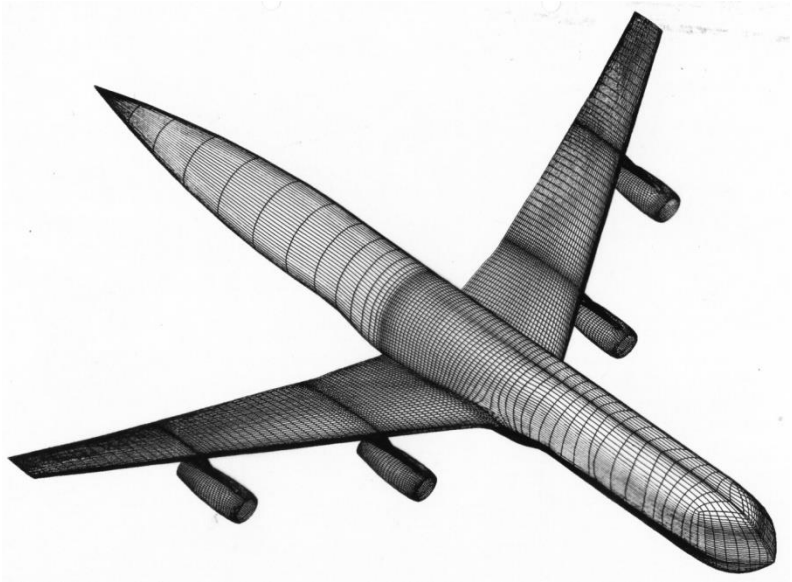

Finite Difference Method

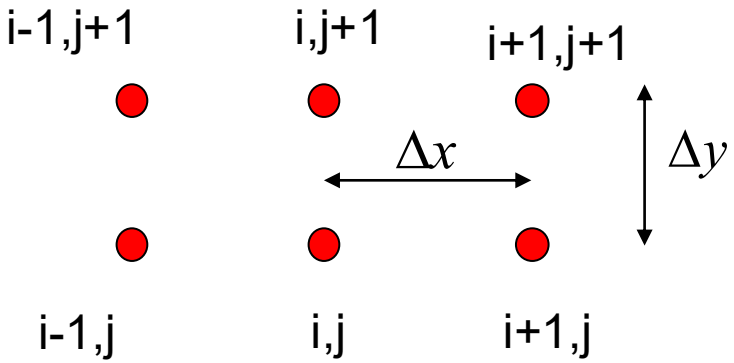

$$\left.\frac{\partial(u\rho)}{\partial x}\right|_{i,j} \approx \frac{((u\rho)_{i+1,j} - (u\rho)_{i-1,j})}{2\Delta x} \qquad O(\Delta x^2)$$

central

$$\left.\frac{\partial(u\rho)}{\partial x}\right|_{i,j} \approx \frac{((u\rho)_{i+1,j} - (u\rho)_{i,j})}{\Delta x} \qquad O(\Delta x)$$

forward

$$\frac{\partial \rho}{\partial t} + \frac{\partial(u\rho)}{\partial x} + \frac{\partial(v\rho)}{\partial y} = 0$$

$$\frac{\partial}{\partial t}\rho_{i,j} + \frac{((u\rho)_{i+1,j} - (u\rho)_{i-1,j})}{2\Delta x} + \frac{((v\rho)_{i,j+1} - (v\rho)_{i,j-1})}{2\Delta y} = 0$$

Finite Volume Method

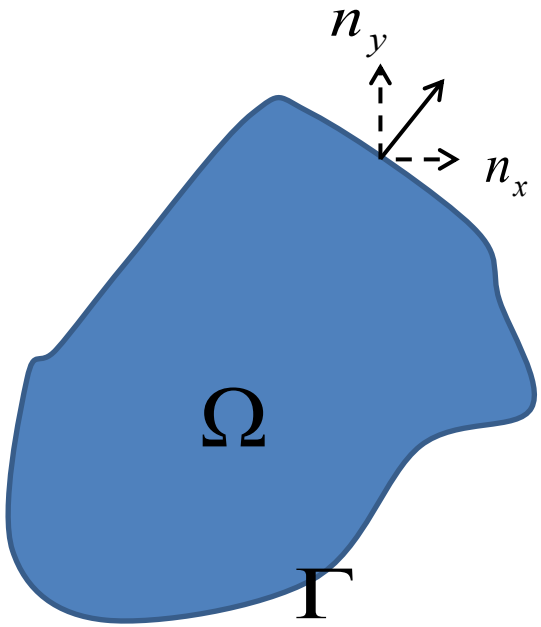

$$\frac{\partial \rho}{\partial t}+\frac{\partial (u\rho)}{\partial x}+\frac{\partial (v\rho)}{\partial y}=0$$

$$\int_\Omega \frac{\partial \rho}{\partial t}d\Omega+\int_\Omega \frac{\partial (u\rho)}{\partial x}d\Omega+\int_\Omega \frac{\partial (v\rho)}{\partial y}d\Omega=0$$

From Gauss Divergence Theorem:

$$\frac{\partial}{\partial t}\int_\Omega \rho d\Omega+\int_\Gamma (u\rho)n_x d\Gamma+\int_\Gamma (v\rho)n_y d\Gamma=0$$

$$\frac{\partial}{\partial t}\rho_i V_i+\sum_j (u\rho)_{ij}\,S_x+\sum_j (v\rho)_{ij}\,S_y=0$$

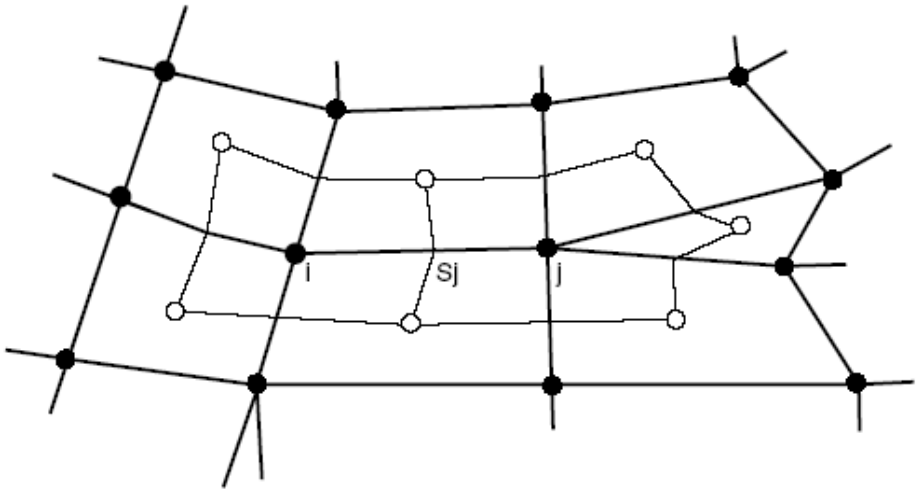

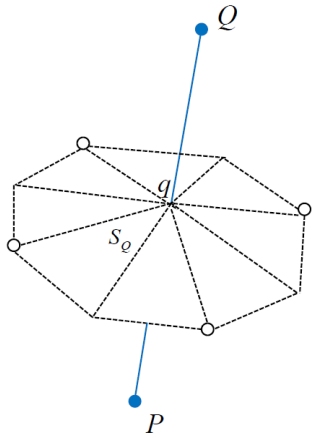

Finite Element Method

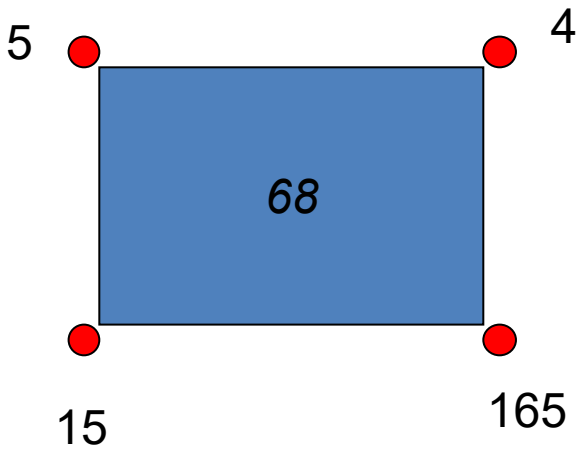

Element	Nodes
68	5 4 165 15

(Repeated index notation is used here)

$$\rho \approx \rho_i N_i =$$

$$\rho_5 N_5 + \rho_4 N_4 + \rho_{165} N_{165} + \rho_{15} N_{15}$$

$$\frac{\partial \rho}{\partial t} + \frac{\partial (u\rho)}{\partial x} + \frac{\partial (v\rho)}{\partial y} = 0$$

$$\int_\Omega \frac{\partial \rho}{\partial t} d\Omega + \int_\Omega \frac{\partial (u\rho)}{\partial x} d\Omega + \int_\Omega \frac{\partial (v\rho)}{\partial y} d\Omega = 0$$

$$\frac{\partial}{\partial t} \int_\Omega \rho_i N_i d\Omega + \int_\Omega \frac{\partial (u\rho)_i N_i}{\partial x} d\Omega + \int_\Omega \frac{\partial (v\rho)_i N_i}{\partial y} d\Omega = 0$$

Finite Element Method continued

Weighted residual analysis:

$$\frac{\partial}{\partial t}\int_\Omega \rho_i N_i W_j d\Omega + \int_\Omega \frac{\partial (u\rho)_i N_i}{\partial x} W_j d\Omega + \int_\Omega \frac{\partial (v\rho)_i N_i}{\partial y} W_j d\Omega = 0$$

$$\frac{\partial}{\partial t}(\int_\Omega N_i W_j d\Omega)\rho_i + (\int_\Omega \frac{\partial (N_i)}{\partial x} W_j d\Omega) u\rho_i + (\int_\Omega \frac{\partial (N_i)}{\partial y} W_j d\Omega) v\rho_i = 0$$

If W is chosen to be the same as N the method is called Galerkin method.

$$\frac{\partial}{\partial t}(\int_\Omega N_i N_j d\Omega)\rho_i + (\int_\Omega \frac{\partial (N_i)}{\partial x} N_j d\Omega) u\rho_i + (\int_\Omega \frac{\partial (N_i)}{\partial y} N_j d\Omega) v\rho_i = 0$$

For easy implementation of boundary conditions this is integrated by parts.

$$\frac{\partial}{\partial t}(\int_\Omega N_i N_j d\Omega)\rho_i - (\int_\Omega N_i \frac{\partial (N_j)}{\partial x} d\Omega) u\rho_i - (\int_\Omega N_i \frac{\partial (N_j)}{\partial y} d\Omega) v\rho_i + (\int_\Gamma N_i N_j n_x d\Gamma) u\rho_i + (\int_\Gamma N_i N_j n_y d\Gamma) v\rho_i = 0$$

$$\frac{\partial}{\partial t}\mathbf{M}_{elem}\rho_i + \mathbf{B}_{Xelem} u\rho_i + \mathbf{B}_{Yelem} v\rho_i = 0$$

Finite Element Method

1) Divides computational space into elements

$$\frac{\partial}{\partial t}\mathbf{M}_{elem}\rho_i + \mathbf{B}_{Xelem}u\rho_i + \mathbf{B}_{Yelem}v\rho_i = 0$$

For every element construct

$$\mathbf{M}_{elem}, \mathbf{B}_{Xelem}, \mathbf{B}_{Yelem}; \boldsymbol{\rho}_{elem}, \mathbf{u}\boldsymbol{\rho}_{elem}, \mathbf{v}\boldsymbol{\rho}_{elem}$$

2) Reconnects elements at nodes

Agglomerates for the whole domain

$$\mathbf{M} = \sum_e \mathbf{M}_{elem}, \mathbf{B}_X = \sum_e \mathbf{B}_{Xelem}, \mathbf{B}_Y = \sum_e \mathbf{B}_{Yelem}$$

$$\boldsymbol{\rho} = \sum_e \boldsymbol{\rho}_{elem}, \mathbf{u}\boldsymbol{\rho} = \sum_e \mathbf{u}\boldsymbol{\rho}_{elem}, \mathbf{v}\boldsymbol{\rho} = \sum_e \mathbf{v}\boldsymbol{\rho}_{elem}$$

3) As a result, a set of algebraic equations is formed, and its solution follows

$$\frac{\partial}{\partial t}\mathbf{M}\ \boldsymbol{\rho} + \mathbf{B}_X\mathbf{u}\boldsymbol{\rho} + \mathbf{B}_Y\mathbf{v}\boldsymbol{\rho} = \mathbf{0}$$

Matrix Agglomeration

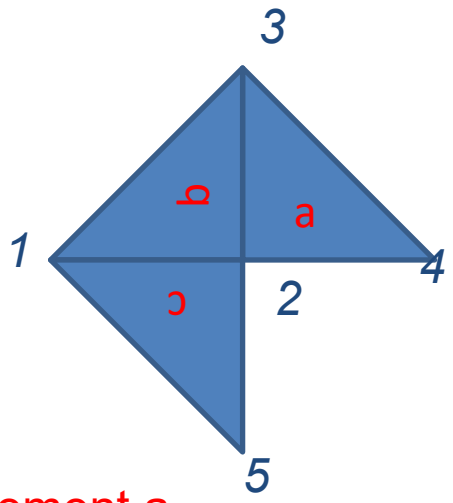

Global matrix is a sum of all element matrixes

$$\begin{bmatrix} b11+c11 & b12+c12 & b13 & 0 & c15 \\ b21+c21 & a22+b22+c22 & a23+b23 & a24 & c25 \\ b31 & a32+b32 & a33+b33 & a34 & 0 \\ 0 & a42 & a43 & a44 & 0 \\ c51 & c52 & 0 & 0 & c55 \end{bmatrix} \begin{bmatrix} \rho 1 \\ \rho 2 \\ \rho 3 \\ \rho 4 \\ \rho 5 \end{bmatrix}$$

Element a

$$\begin{bmatrix} a22 & a23 & a24 \\ a32 & a33 & a34 \\ a42 & a43 & a44 \end{bmatrix} \begin{bmatrix} \rho 2 \\ \rho 3 \\ \rho 4 \end{bmatrix}$$

Element b

$$\begin{bmatrix} b11 & b12 & b13 \\ b21 & b22 & b23 \\ b31 & b32 & b33 \end{bmatrix} \begin{bmatrix} \rho 1 \\ \rho 2 \\ \rho 3 \end{bmatrix}$$

Element c

$$\begin{bmatrix} c11 & c12 & c15 \\ c21 & c22 & c25 \\ c51 & c52 & c55 \end{bmatrix} \begin{bmatrix} \rho 1 \\ \rho 2 \\ \rho 5 \end{bmatrix}$$

$$\frac{\partial}{\partial t}\mathbf{M}\,\boldsymbol{\rho} + \mathbf{B}_X \mathbf{u}\boldsymbol{\rho} + \mathbf{B}_Y \mathbf{v}\boldsymbol{\rho} = \mathbf{0}$$

e.g. For the linear triangular element the consistent mass matrix

$$\begin{bmatrix} a22 & a23 & a24 \\ a32 & a33 & a34 \\ a42 & a43 & a44 \end{bmatrix} = \begin{bmatrix} 2 & 1 & 1 \\ 1 & 2 & 1 \\ 1 & 1 & 2 \end{bmatrix} \cdot \frac{\text{Area Element"a"}}{12}$$

SHAPE FUNCTIONS

$$\rho \approx \sum_i N_i \rho_i$$

And when derivatives are of interest:

$$\frac{d\rho}{dx} \approx \sum_i \frac{dN_i}{dx} \rho_i$$

The tetrahedron family of elements

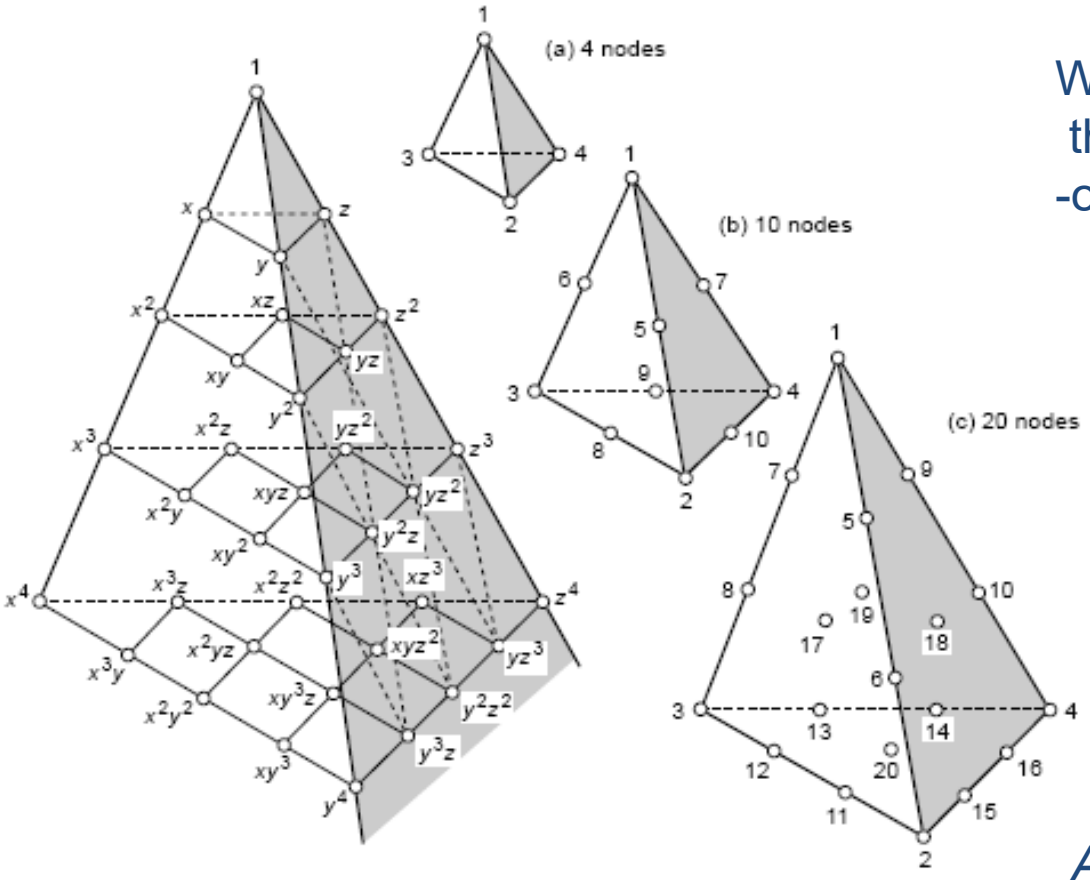

We know functions N,
they are frequently polynomials
-obtaining their derivatives is easy.

After Zienkiewicz et al FEM 2000

SHAPE FUNCTIONS

Example: a linear interpolation of a scalar T in a triangle. The value of T in an arbitrary point alpha is approximated by:

$$\rho_\alpha \approx \rho_1 N_1 + \rho_2 N_2 + \rho_3 N_3$$

$$N_1 = A_1 / A_{element}$$

where A is an area

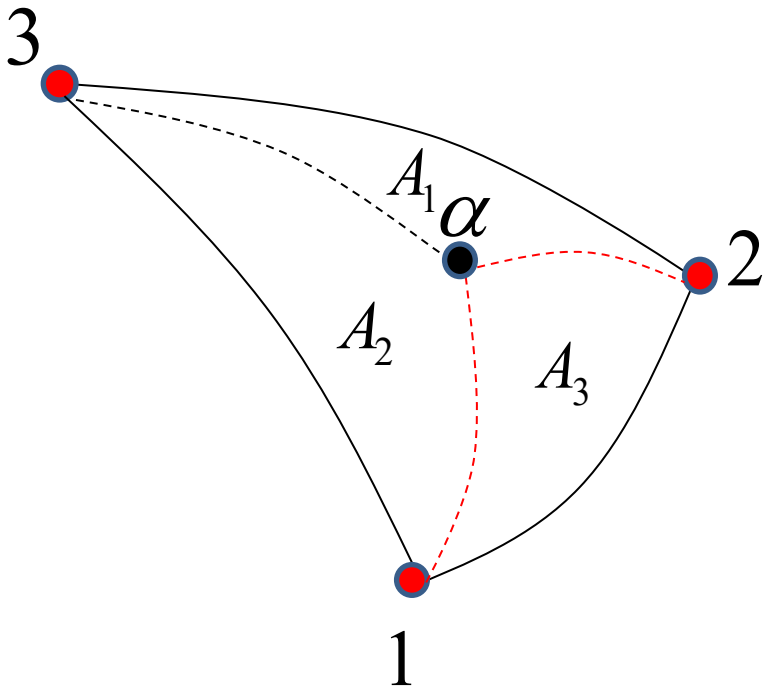

SHAPE FUNCTIONS

Curvilinear elements can be formed using transformations

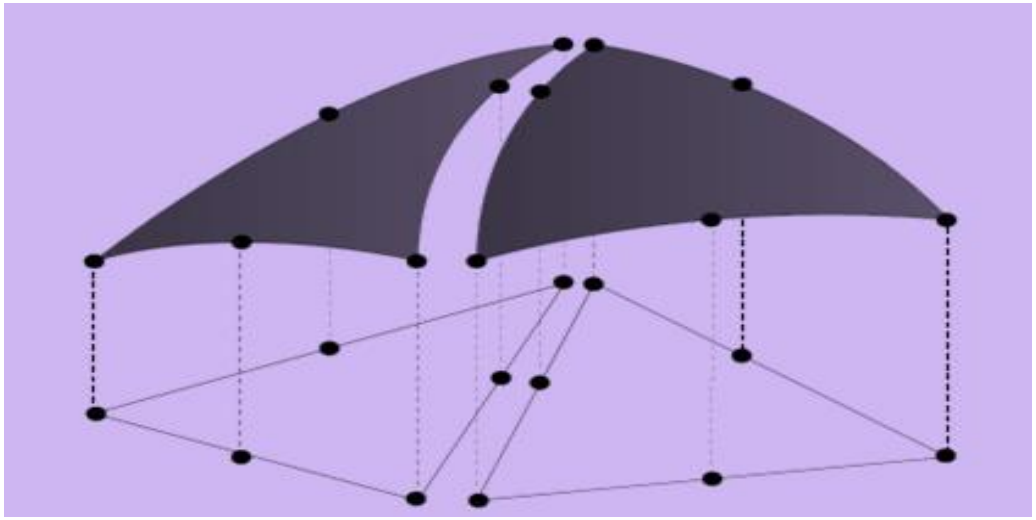

Isoparametric elements

Typical Examples of Data Structures

Structured

Point based --- I,J,K indexing
Set of coordinates and connectivities
Naturally map into the elements of a matrix

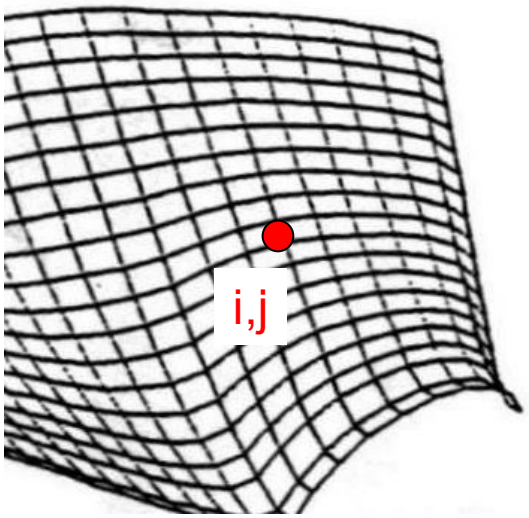

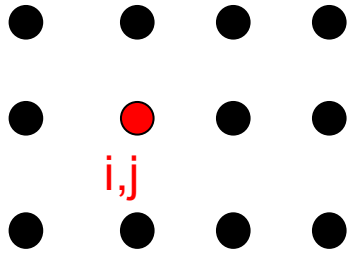

Typical Examples of Data Structures

Structured

Binary trees

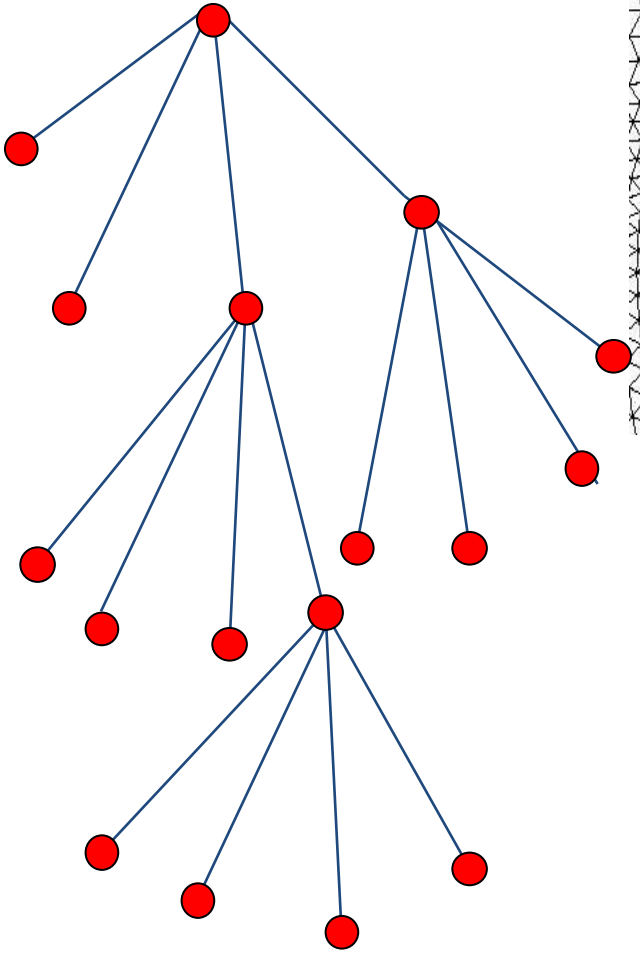

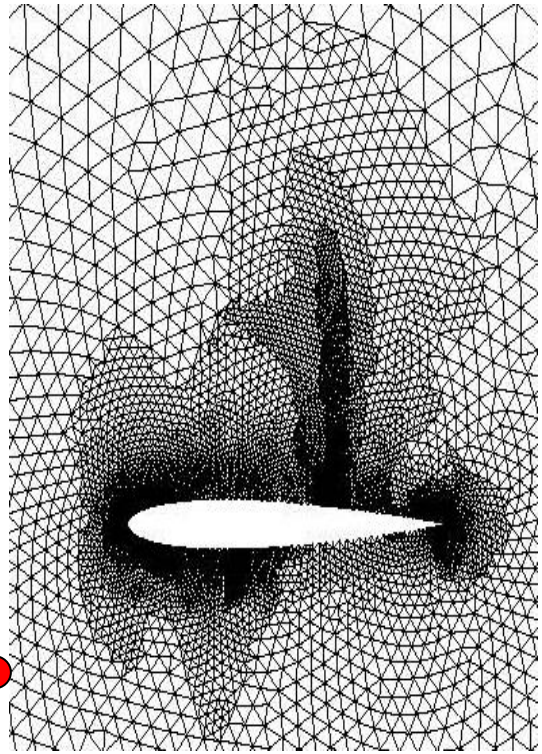

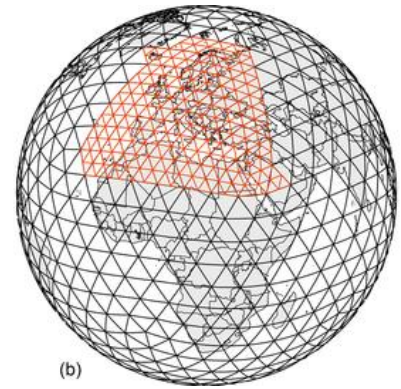

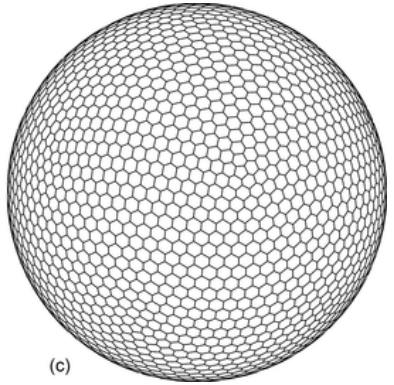

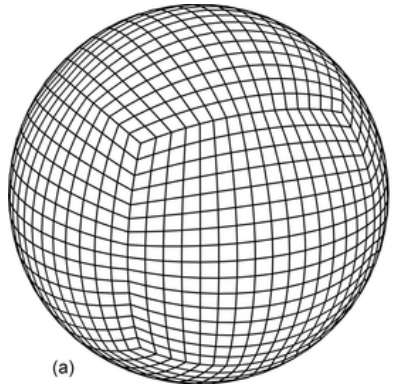

Source: Ullrich et al GMD 2017

Typical Examples of Data Structures

Unstructured

Element based connectivity

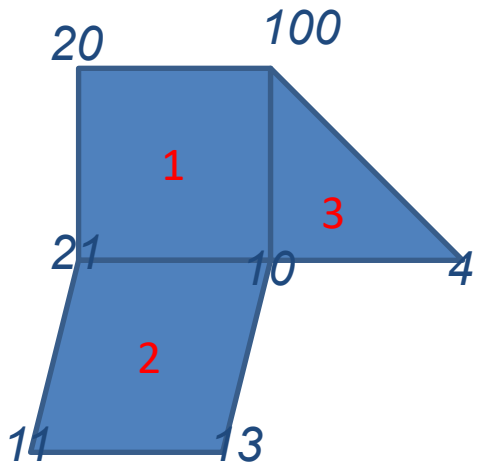

Element 1	10 100 20 21
Element 2	21 11 13 10
Element 3	4 100 10

+ information related to shape functions

Typical Examples of Data Structures

Unstructured

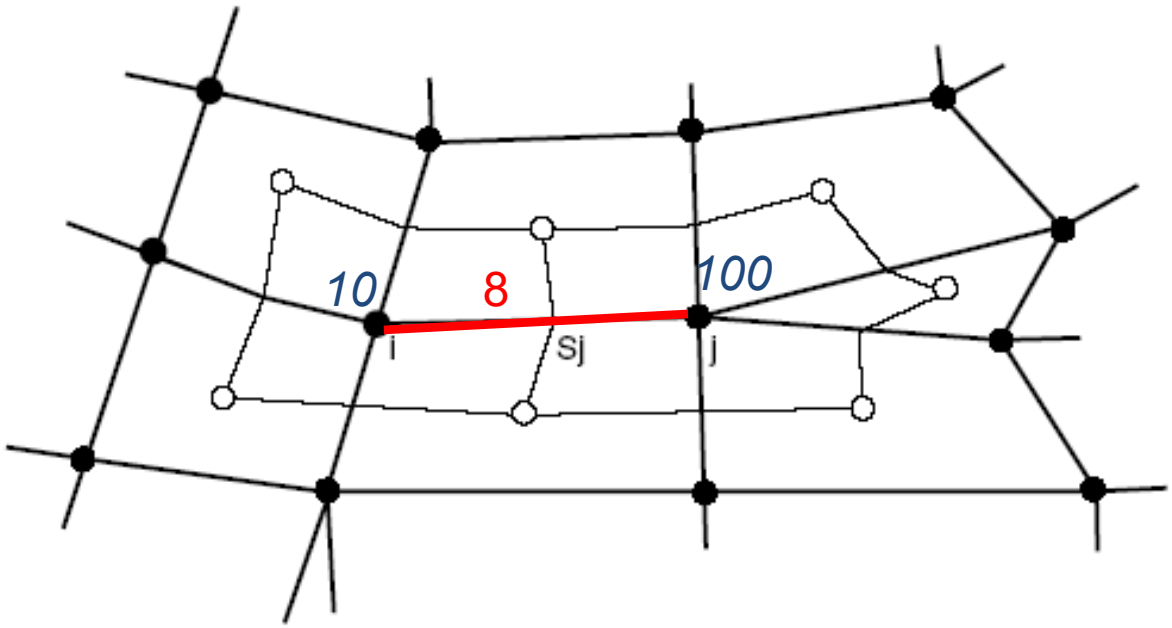

Edge 8 10 100

+ geometrical information

Edge based data

☺ *Flexible mesh adaptivity and hybrid meshes*

☺ *Low storage*

☺ *Easy generalisation to 3D,*

☺ *Less expensive than element based data structure*

More expensive operations than I,J,K

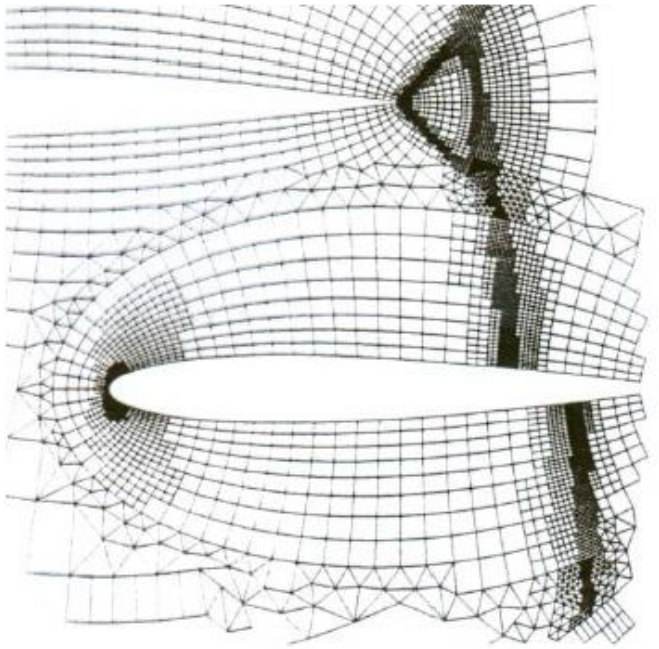

Selected Mesh Generation Techniques

Unstructured Meshes

Direct triangulation

Advancing Front Technique

Delaunay Triangulation

Others

Structured Meshes

Cartesian grids with mapping and/or immersed boundaries

Variants of icosahedral meshes

Others

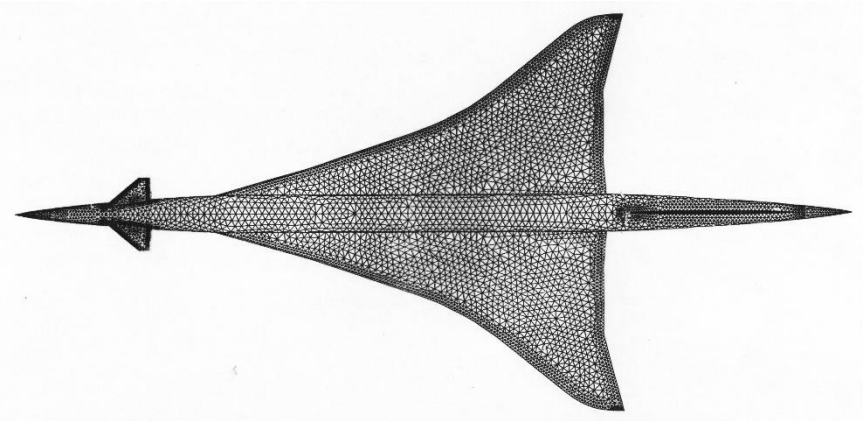

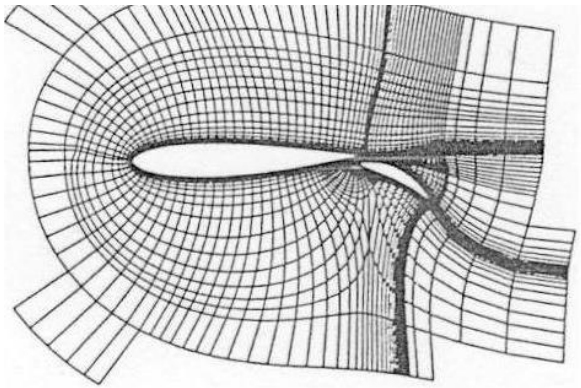

An example of the direct triangulation

Reduced Gaussian Grid

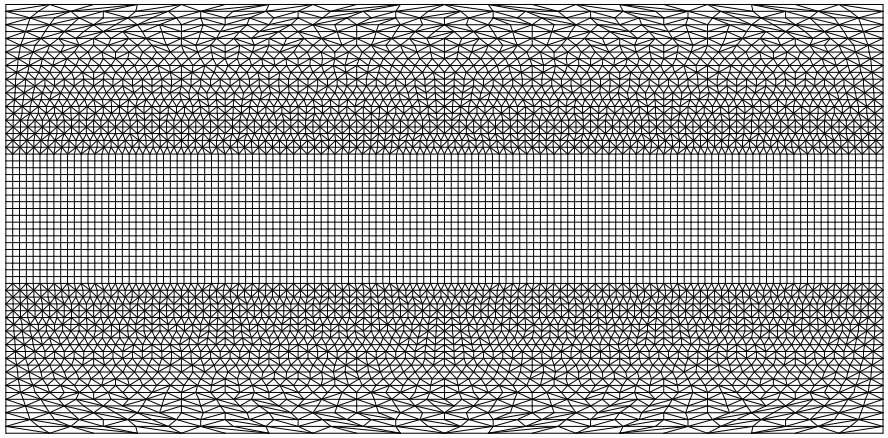

Primary mesh

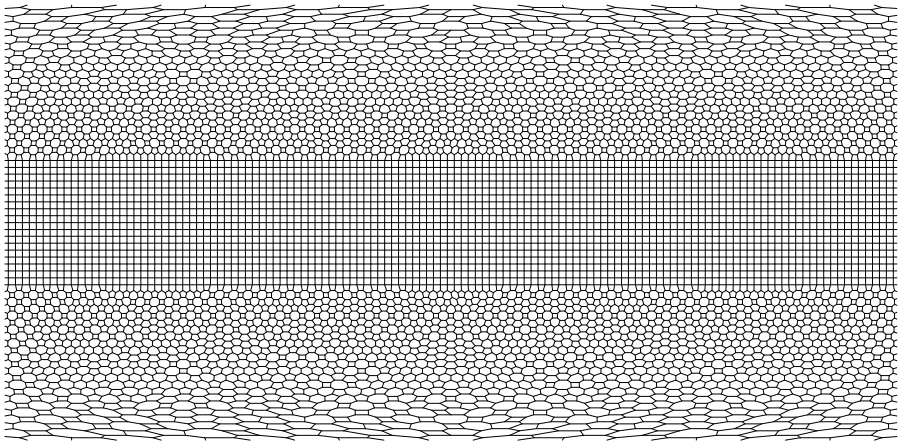

Dual mesh

Rossby-Haurwitz Wave

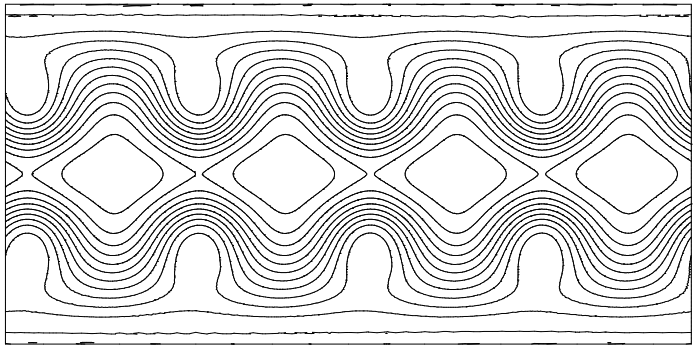

5 days

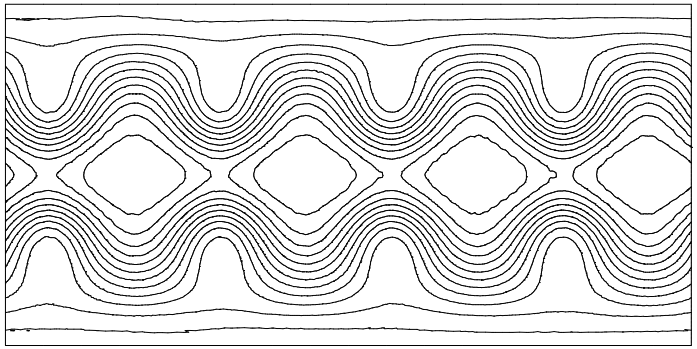

14 days

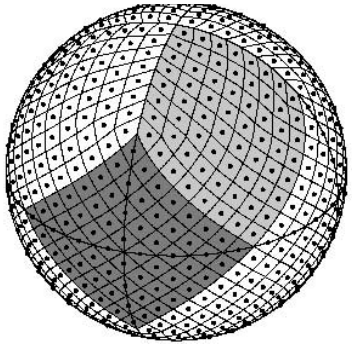

An example of bespoke mesh

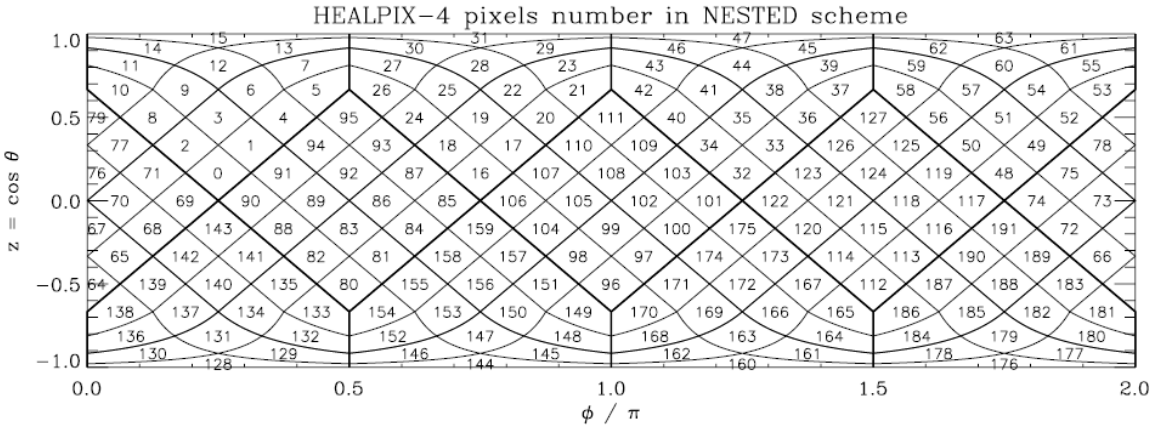

Source: Gorski et al
Astrophysical Journal 2005

Oct.N80 and reduced meshes

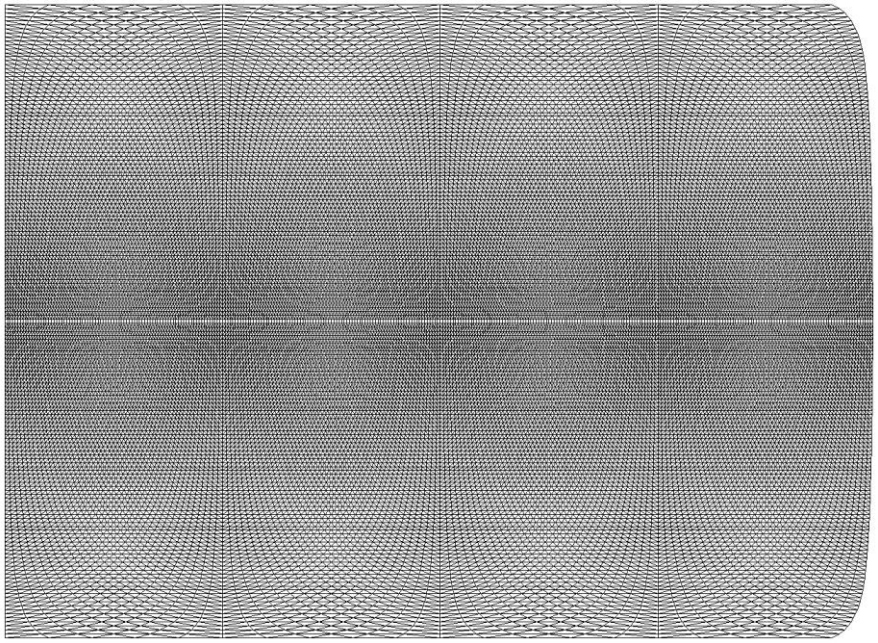

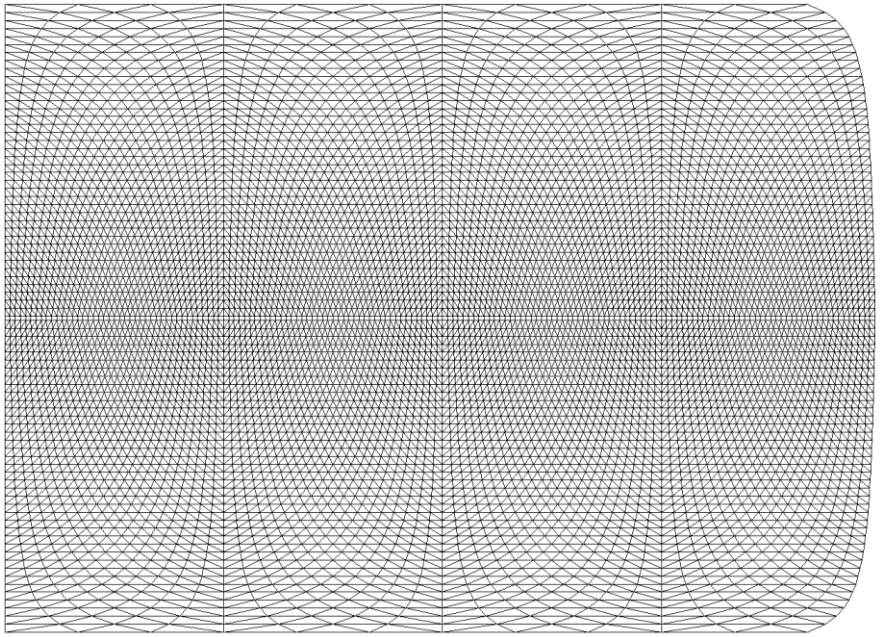

Oct.N80 fine and ‘odd’ reduced meshes

Reduced Mesh – Baroclinic Instability

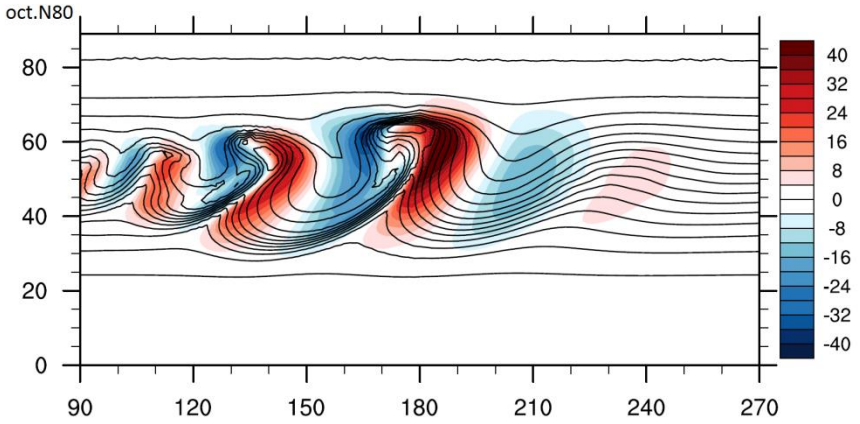

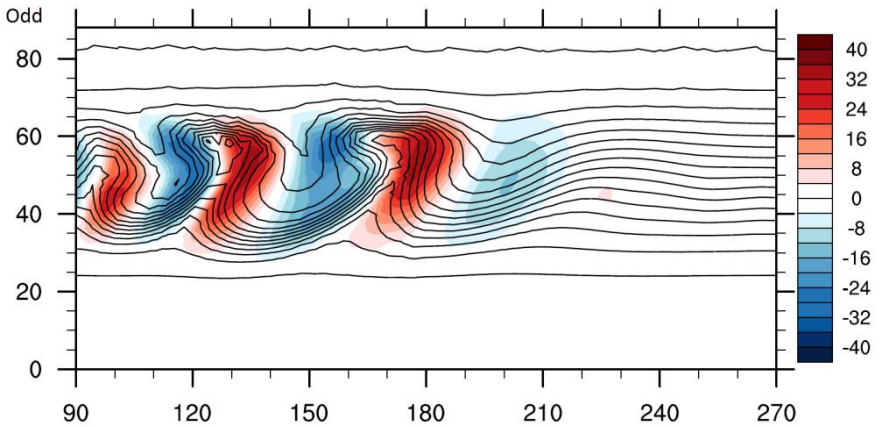

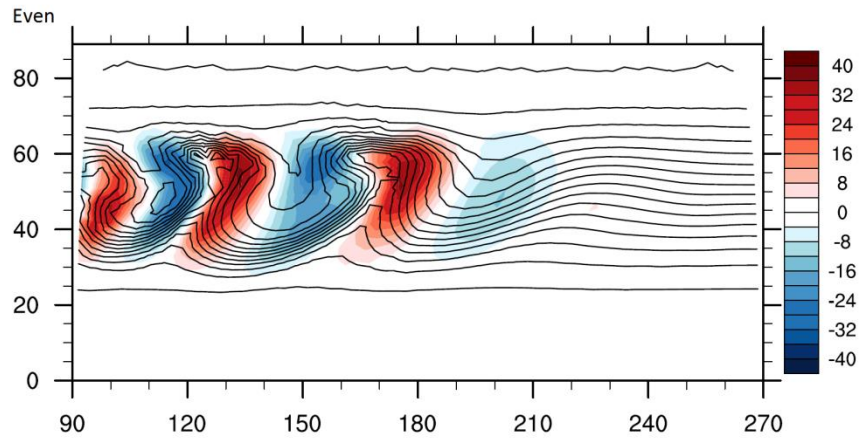

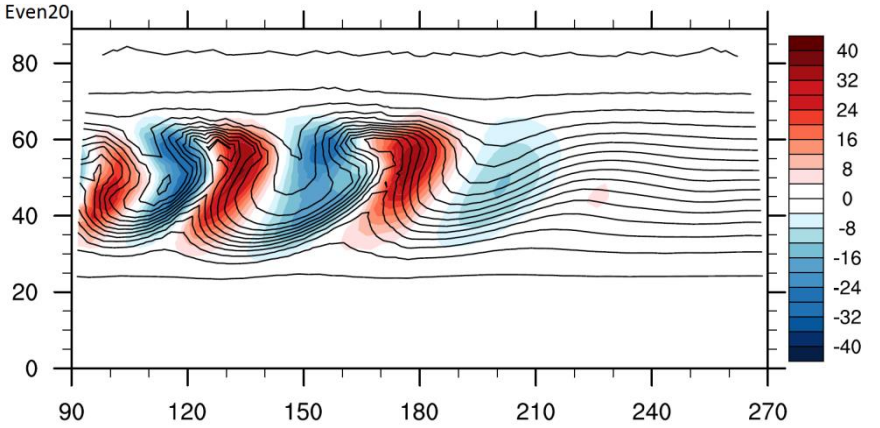

Day 8, horizontal velocity and potential temperature

Advancing Front Technique

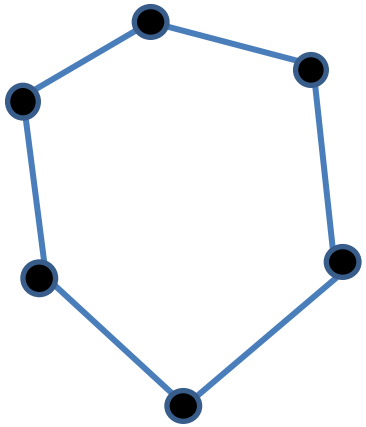

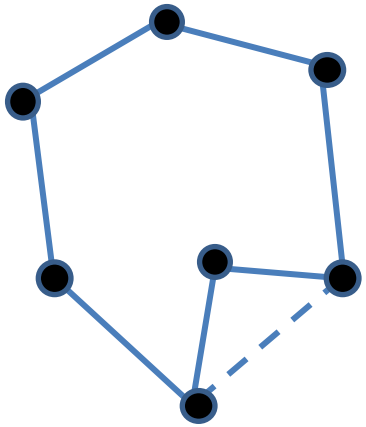

Simultaneous mesh point generation and connectivity

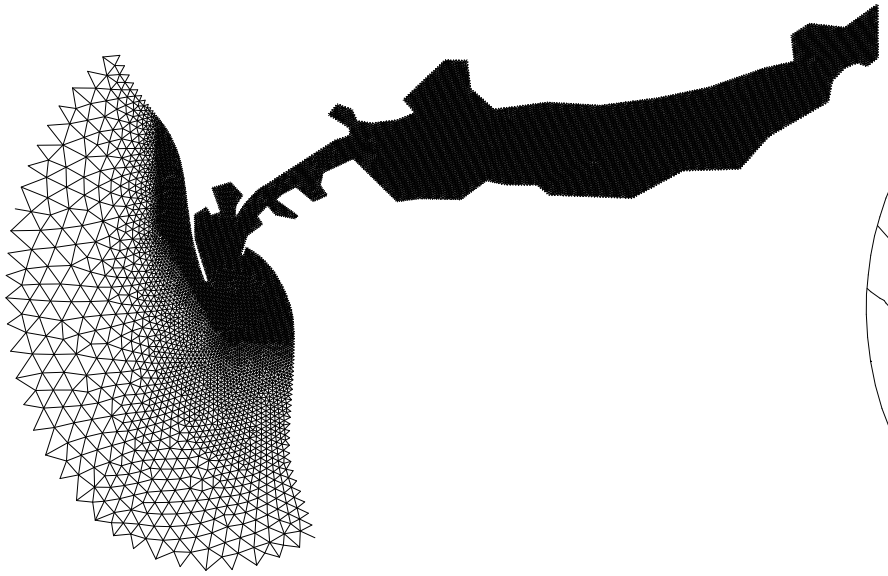

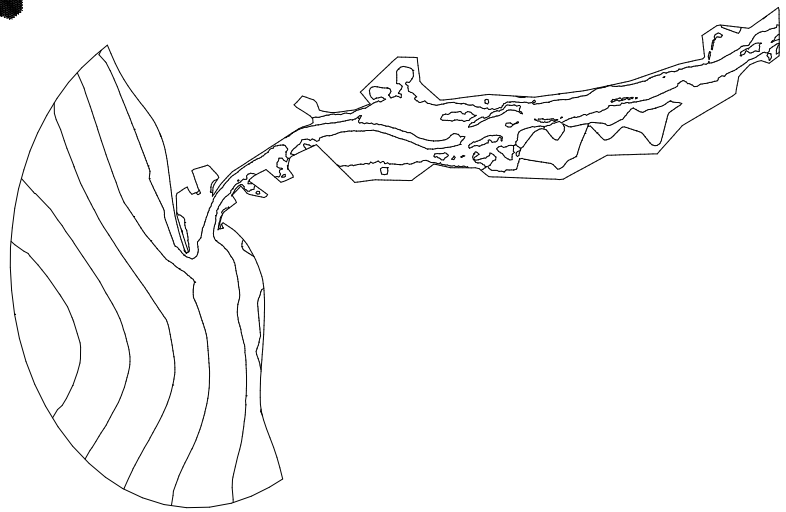

Delaunay Triangulation

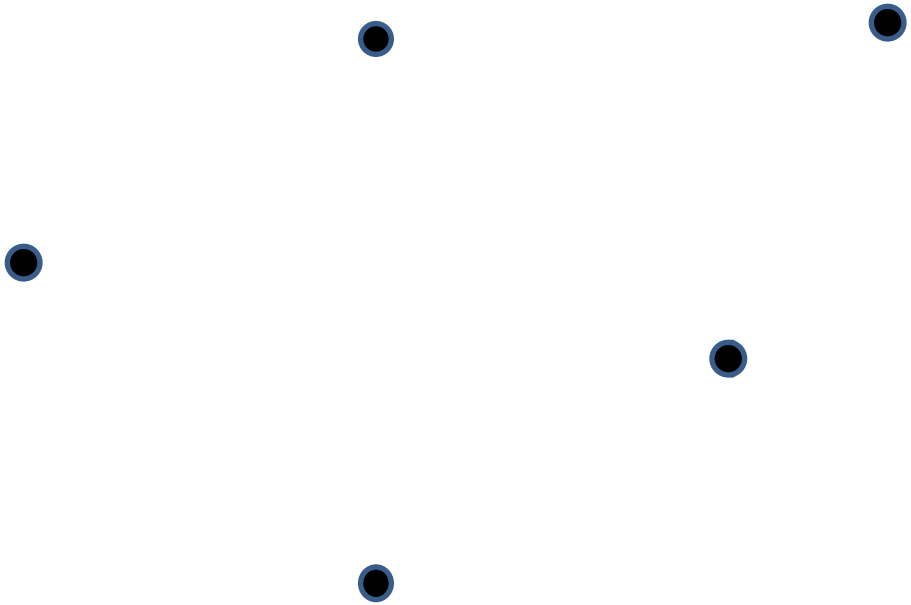

How to connect a given set of points?

Delaunay Triangulation

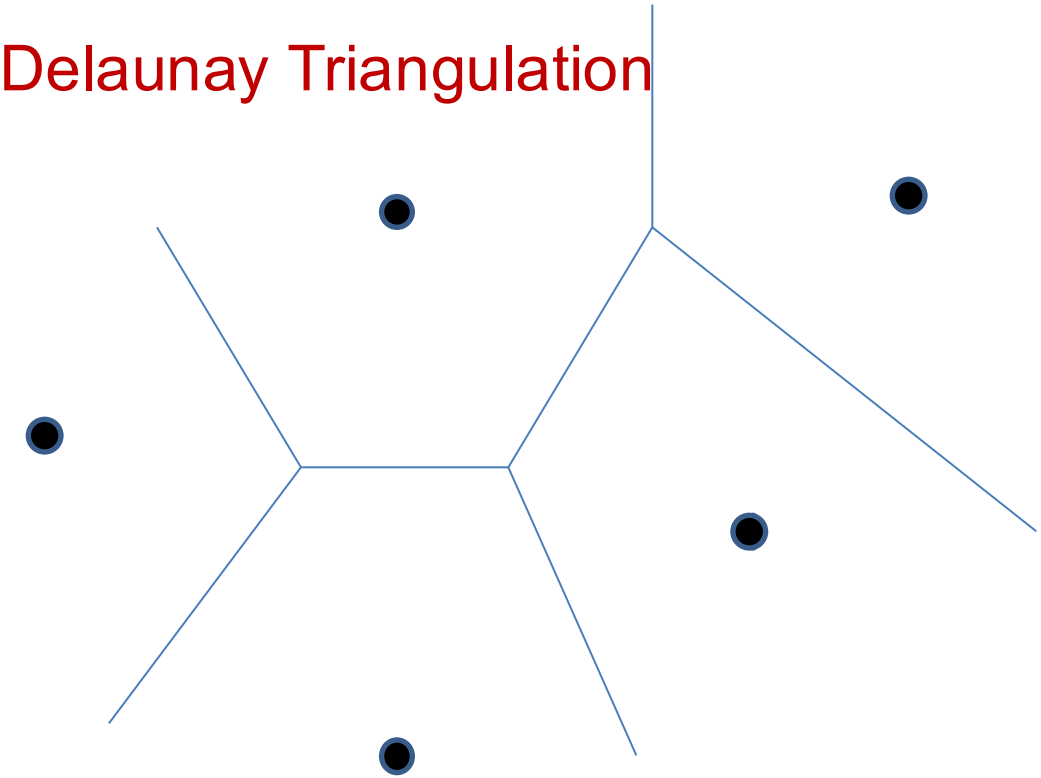

Create Voronoi polygons, i.e.
The construct that assigns to each point the area
of the plane closer to that point than to any other point
in the set. A side of a Voronoi polygon must be midway between the two points
which it separates

Delaunay Triangulation

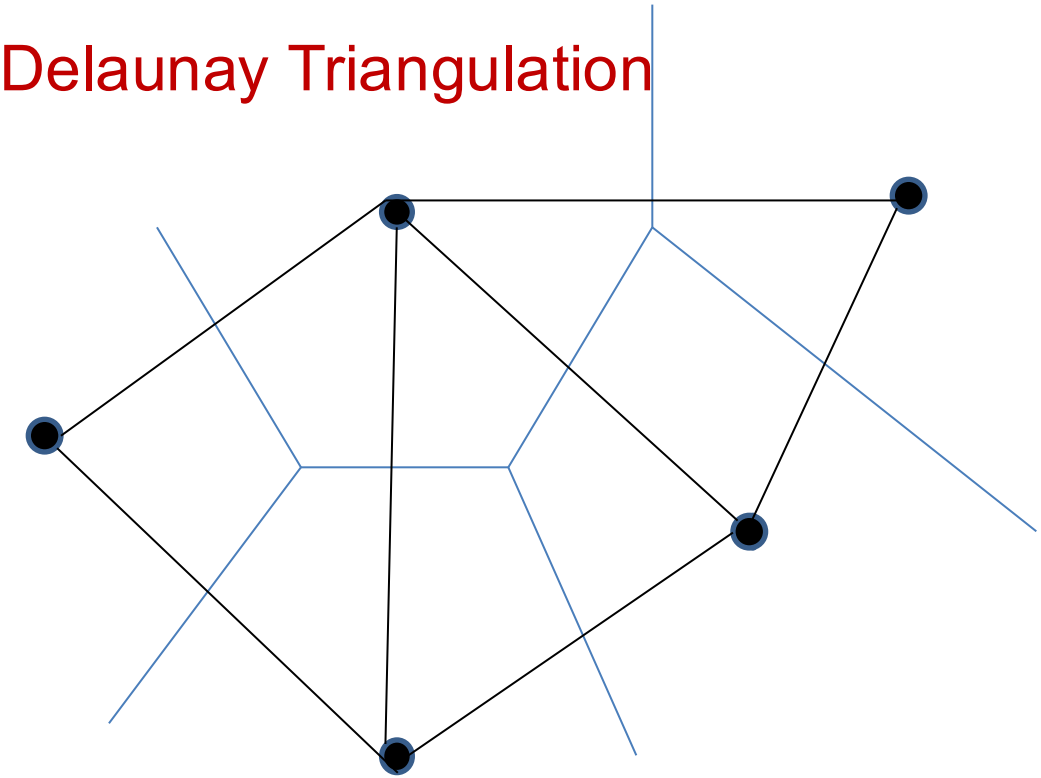

If all point pairs of which have some boundary in common are joint by straight lines, the result is a triangulation of the convex hull of the points.

Delaunay Triangulation mesh constructed from the reduced Gaussian grid points

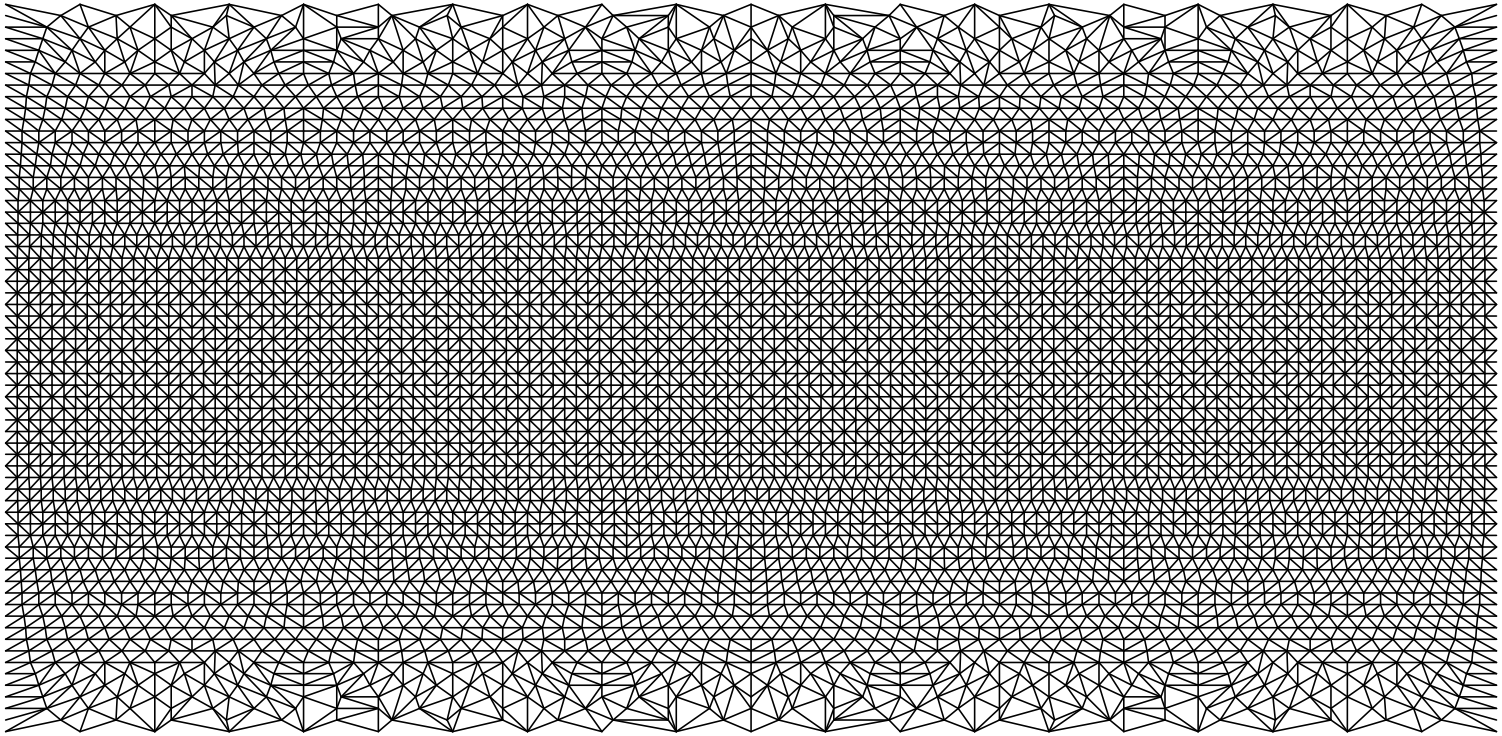

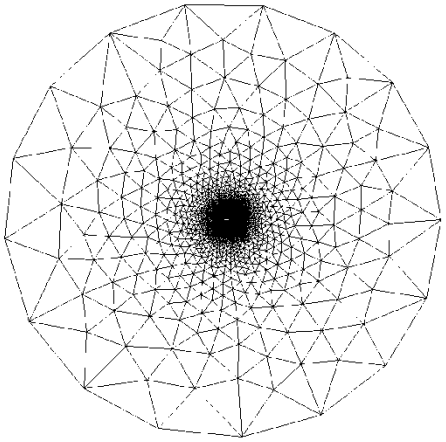

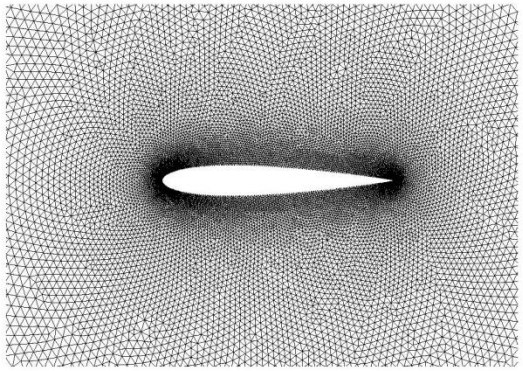

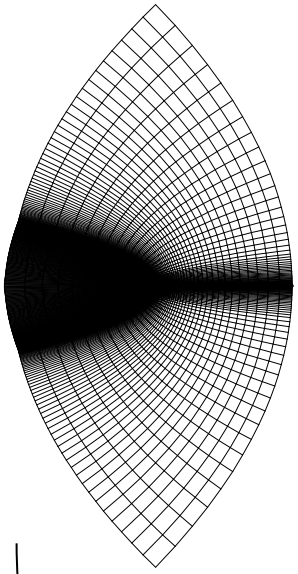

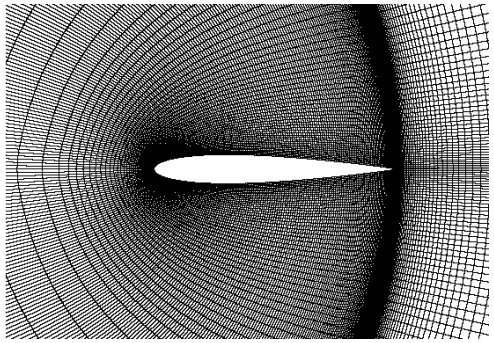

Geometry conforming meshes

Fluxes can be constructed for the surfaces which cut cells

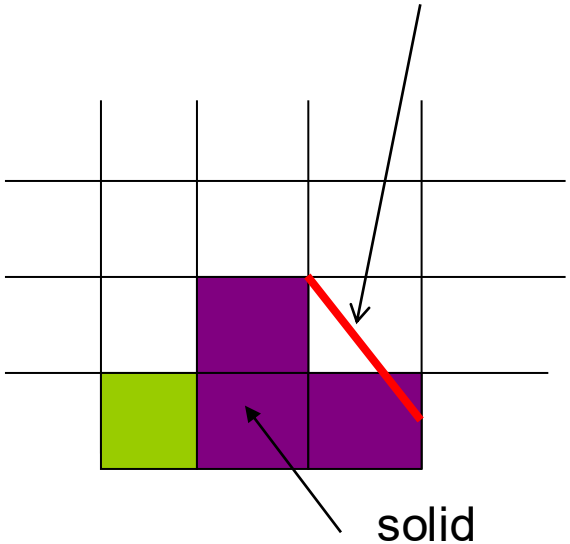

Meshing techniques for mesh adaptivity

-for lower order elements are:

point enrichment (h-refinement),

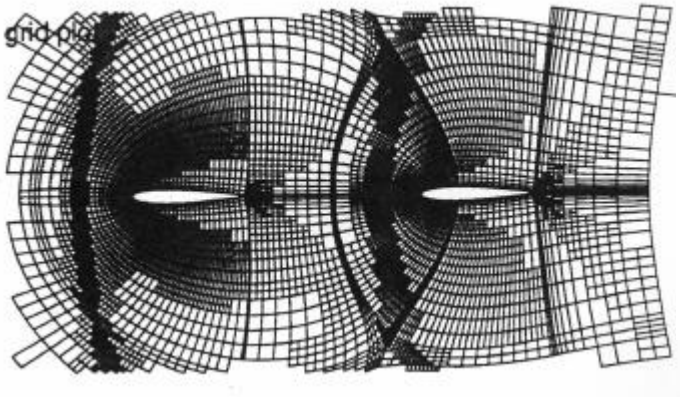

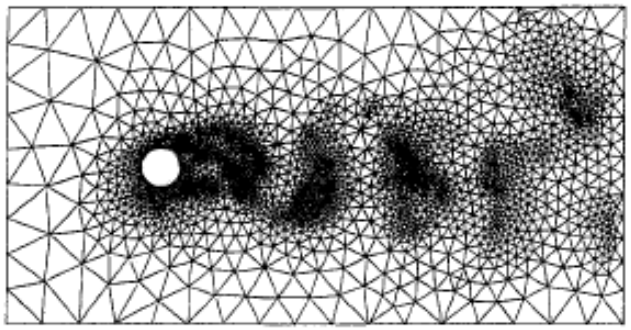

and automatic regeneration

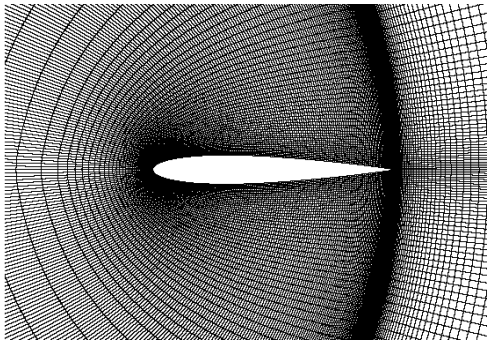

mesh movement

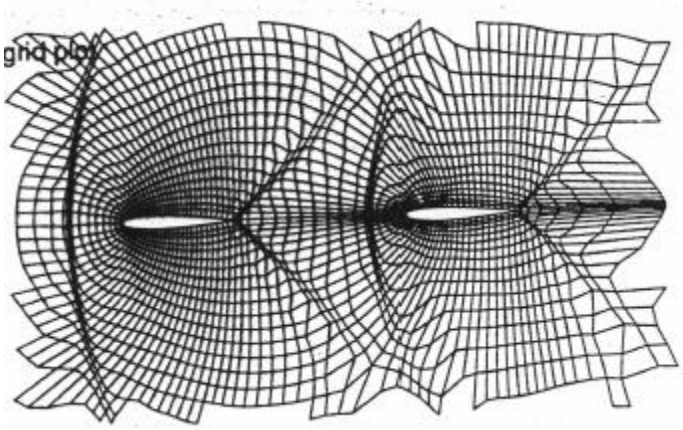

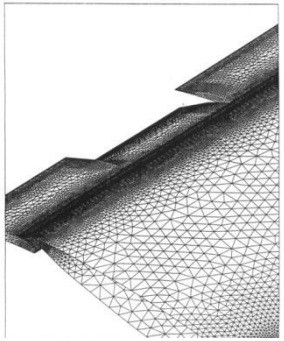

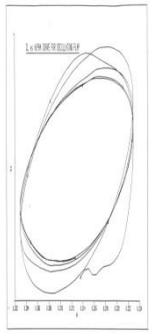

Dynamic regenerations for Meshes utilising a mapping are particularly efficient

-for higher order elements
(p-refinement) increases order of shape function that is the order of **p**olynomial used for elemental interpolation

The Edge Based Finite Volume Discretisation

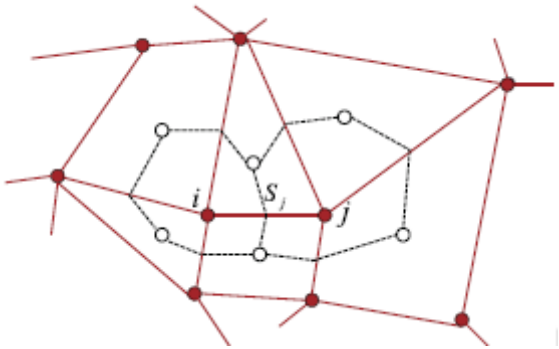

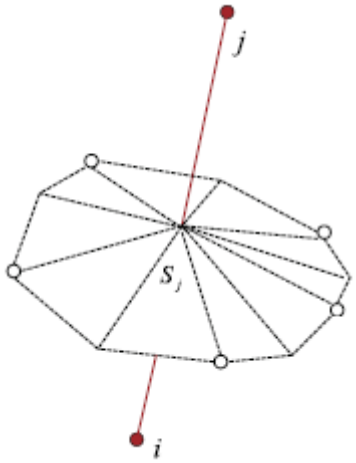

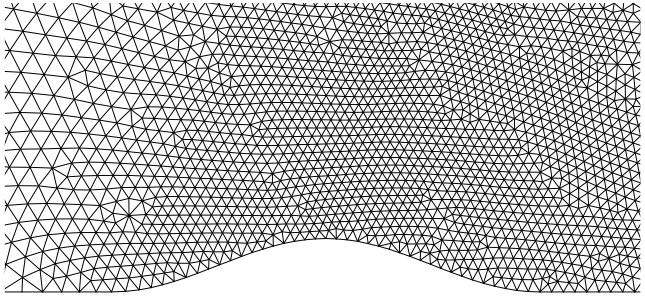

Edges

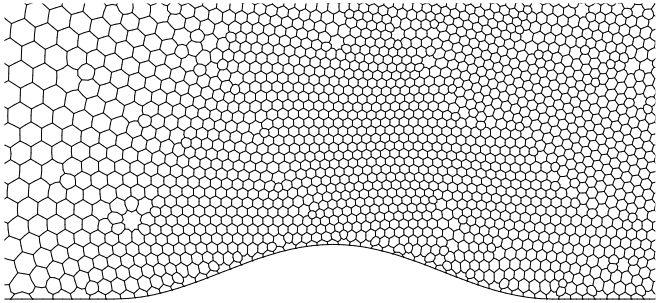

Median dual computational mesh
Finite volumes

Geospherical framework

$$\frac{\partial G\Phi}{\partial t} + \nabla \cdot (\mathbf{V}\Phi) = GR$$

$$\Phi_i^{n+1} = \mathcal{A}_i(\Phi^n + 0.5\delta t R^n,\ \mathbf{V}^{n+1/2}, G) + 0.5\delta t R_i^{n+1}$$

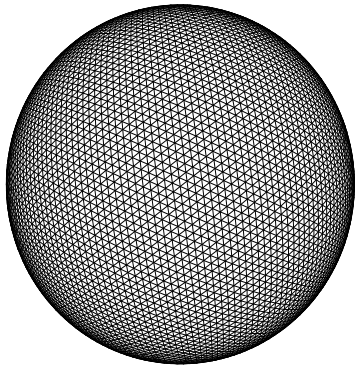

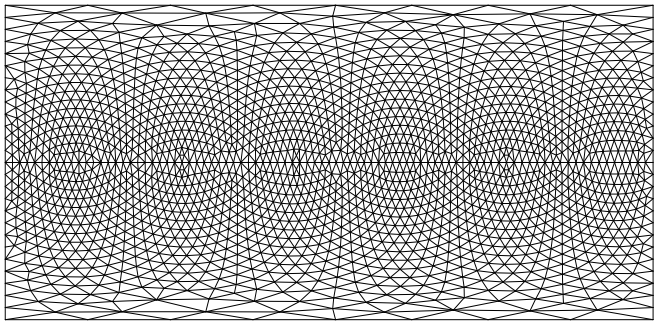

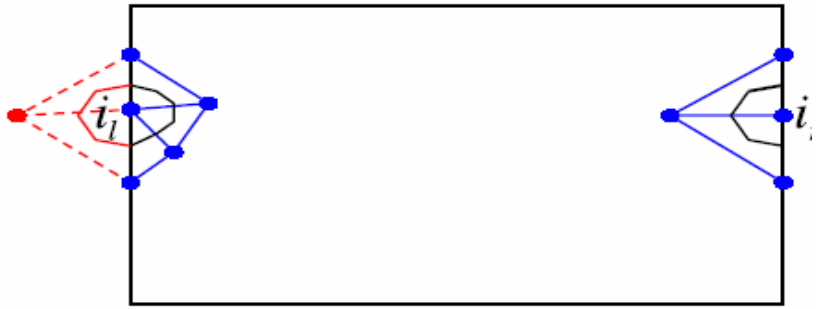

(Szmelter & Smolarkiewicz, J. Comput. Phys. 2010)

A stratified 3D mesoscale flow past an isolated hill

$$h(x,y) = h_0[1. + (l/\mathcal{L})^2]^{-3/2},$$

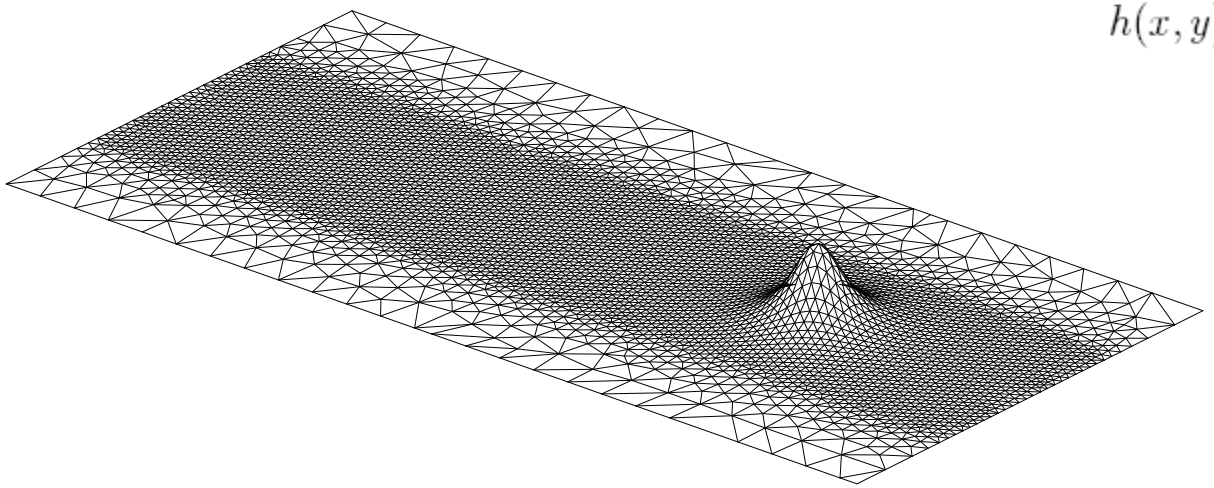

(4532 points)

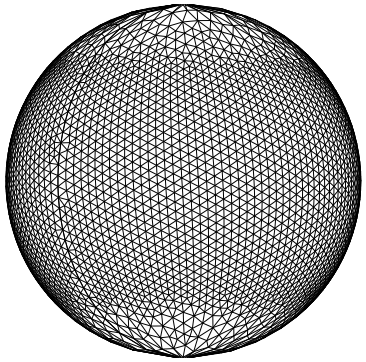

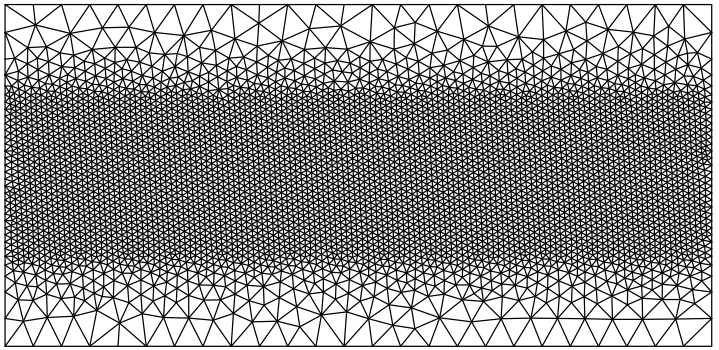

Reduced planets (Wedi & Smolarkiewicz, QJR 2009)

Stratified (mesoscale) flow past an isolated hill on a reduced planet

4 hours

$$Fr = U_0/Nh$$

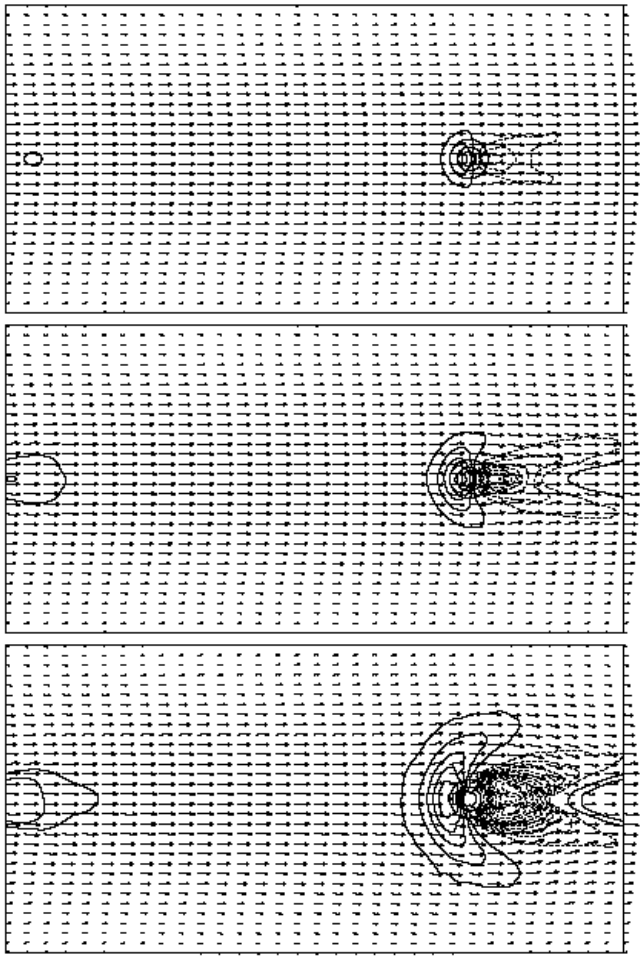

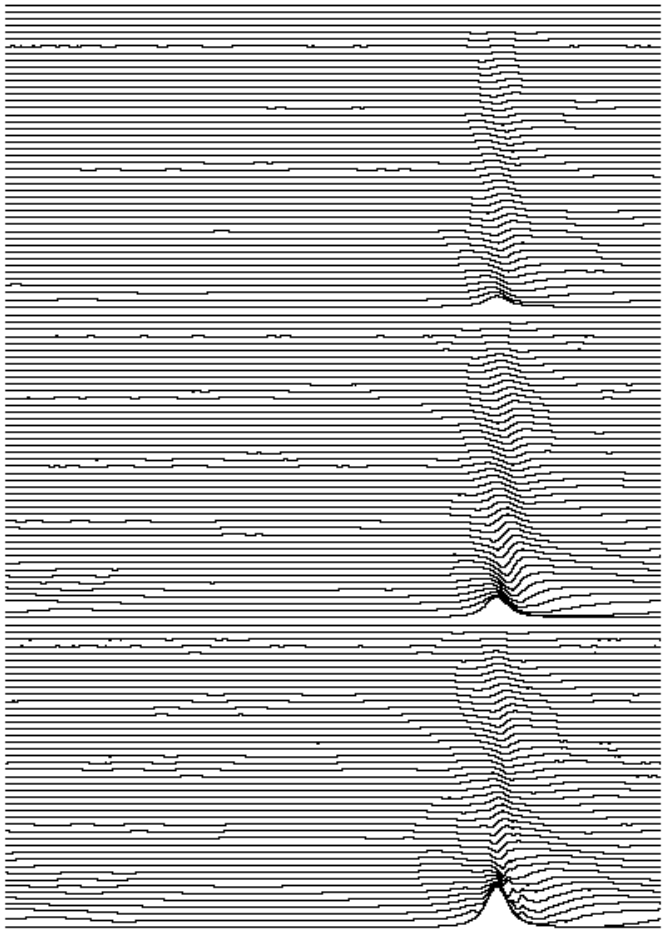

Hunt & Snyder J. Fluid Mech. 1980; Smolar. & Rotunno, J. Atmos. Sci. 1989 ; Wedi & Smolar., QJR 2009

Fr=0.5

$Ro \gg 1$ $Ro \gtrsim 1$

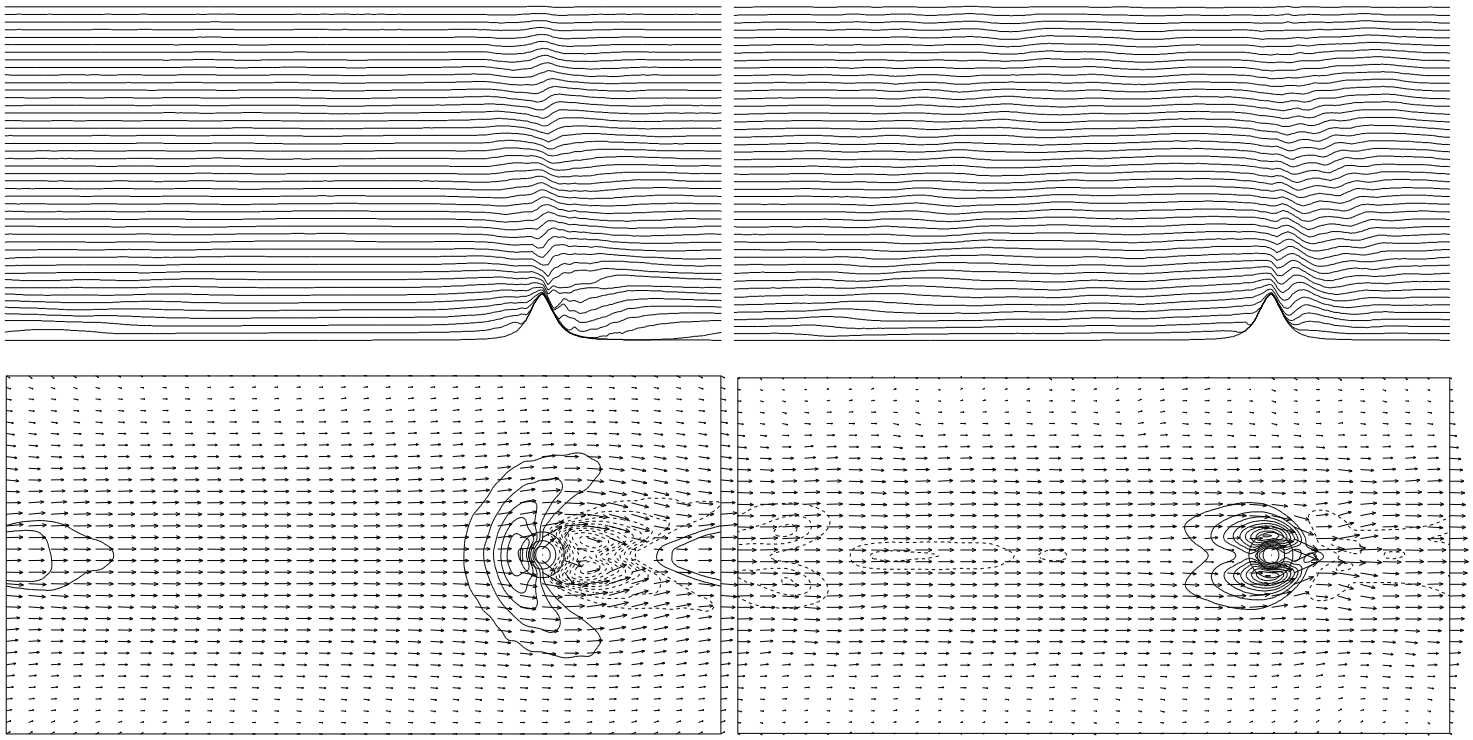

Smith, Advances in Geophys 1979; Hunt, Olafsson & Bougeault, QJR 2001

Multigrid techniques

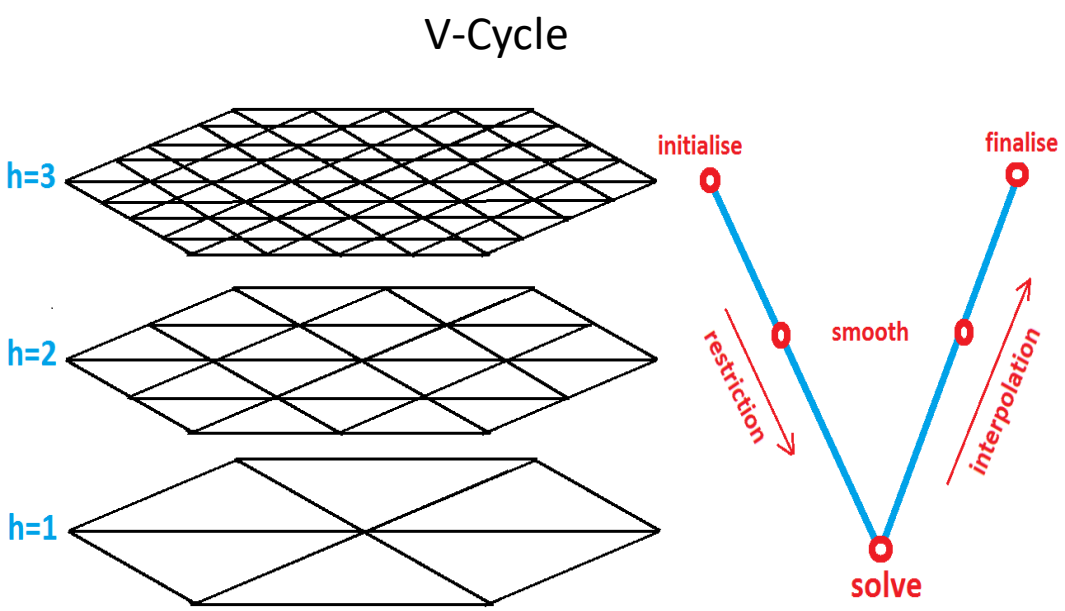

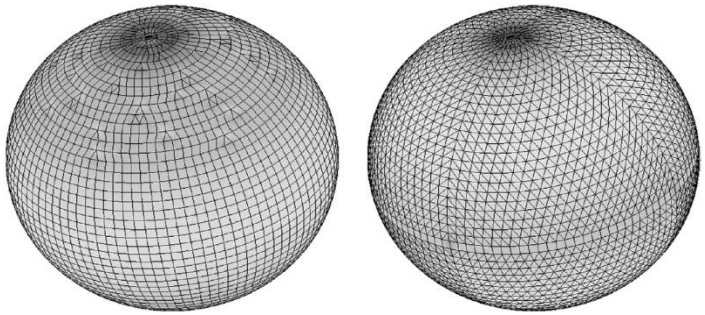

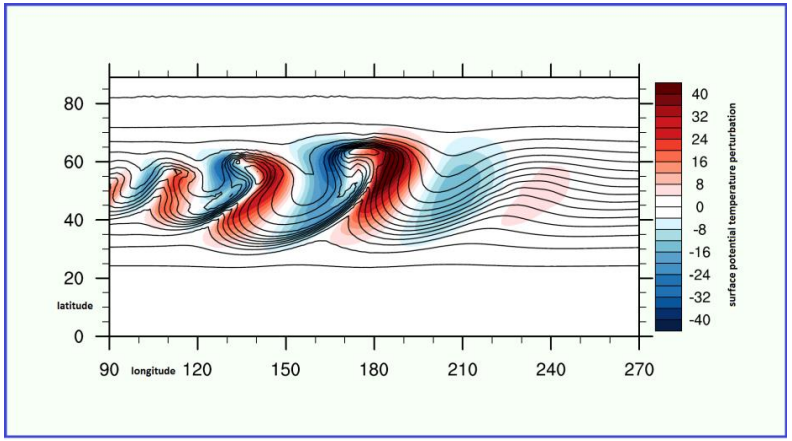

Multigrid using Atlas

Octahedral 16 mesh:

computational domain

Remove odd latitudes

Single level of mesh coarsening

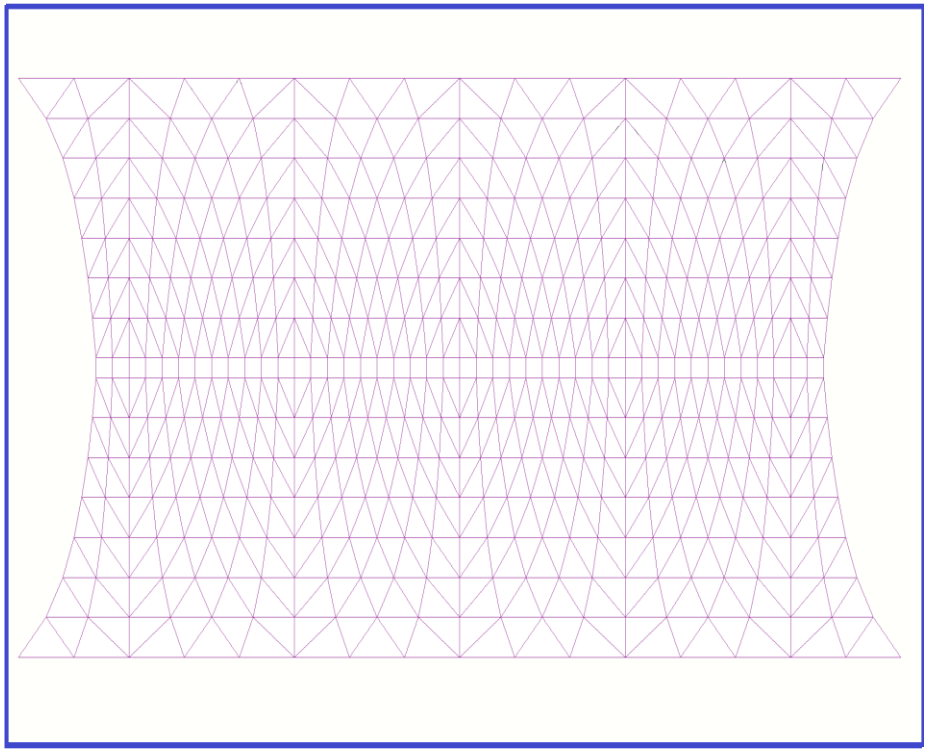

Nonhydrostatic Boussinesq mountain wave

Szmelter & Smolarkiewicz , *Comp. Fluids*, 2011

$$\nabla \bullet (\mathbf{V}\rho_o) = 0 \ ,$$

$$\frac{\partial \rho_o V^I}{\partial t} + \nabla \bullet (\mathbf{V}\rho_o V^I) = -\rho_o \frac{\partial \tilde{p}}{\partial x^I} + g\rho_o \frac{\theta'}{\theta_o}\delta_{I2}$$

$$\frac{\partial \rho_o \theta}{\partial t} + \nabla \bullet (\mathbf{V}\rho_o \theta) = 0 \ .$$

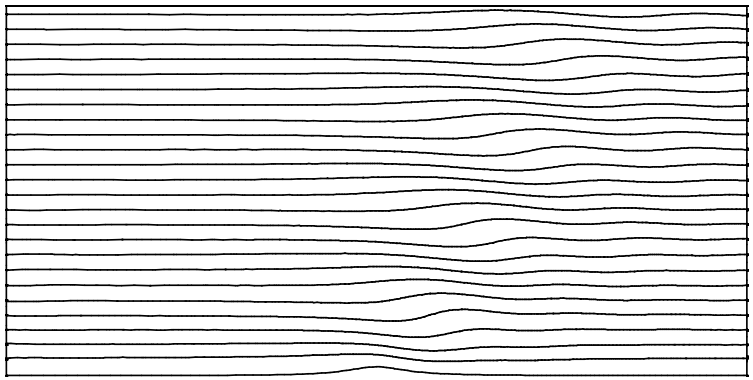

$NL/U_o = 2.4$

Comparison with the EULAG's (structured mesh) results --- very close with the linear theories (Smith 1979, Durran 2003):

over 7 wavelenghts : 3% in wavelength; 8% in propagation angle; wave amplitude loss 7%

$$\frac{\partial \mathbf{\Phi}}{\partial t} + \nabla \bullet (\mathbf{V}\mathbf{\Phi}) = \mathbf{R}$$

Gravity wave breaking in an isothermal stratosphere

$$\nabla \cdot (\bar{\rho}\mathbf{v}) = 0\,, \quad \frac{D\theta}{Dt} = 0\,, \quad \frac{D\mathbf{v}}{Dt} = -\nabla\Phi' - \mathrm{g}\frac{\theta'}{\bar{\theta}}\,,$$ *Lipps & Hemler*

$$\nabla \cdot (\bar{\rho}\bar{\theta}\mathbf{v}) = 0\,, \quad \frac{D\theta}{Dt} = 0\,, \quad \frac{D\mathbf{v}}{Dt} = -c_p\theta\nabla\pi' - \mathrm{g}\frac{\theta'}{\bar{\theta}}$$ *Durran*

$$D\psi/Dt = R$$

by combining $\rho^* \cdot \left(D\psi/Dt = R\right)$ with $\psi \cdot \left(\nabla\rho^*\mathbf{v} = 0\right)$,

$$\frac{\partial \rho^*\psi}{\partial t} + \nabla \cdot (\rho^*\mathbf{v}\psi) = \rho^* R\,.$$

$$\psi_i^{n+1} = \mathcal{A}_i(\bar{\psi}, \mathbf{v}^{n+1/2}, \rho^*) + 0.5\delta t R_i^{n+1}$$

$$S_\theta = d\ln\bar{\theta}/dz = 4.4 \cdot 10^{-5}\ \mathrm{m}^{-1}$$
$$\mathbf{v}_e = (u_e, 0) \quad u_e = U = 20\mathrm{ms}^{-1}$$

Isentropes at $t = 60$, 90, and 120 min.

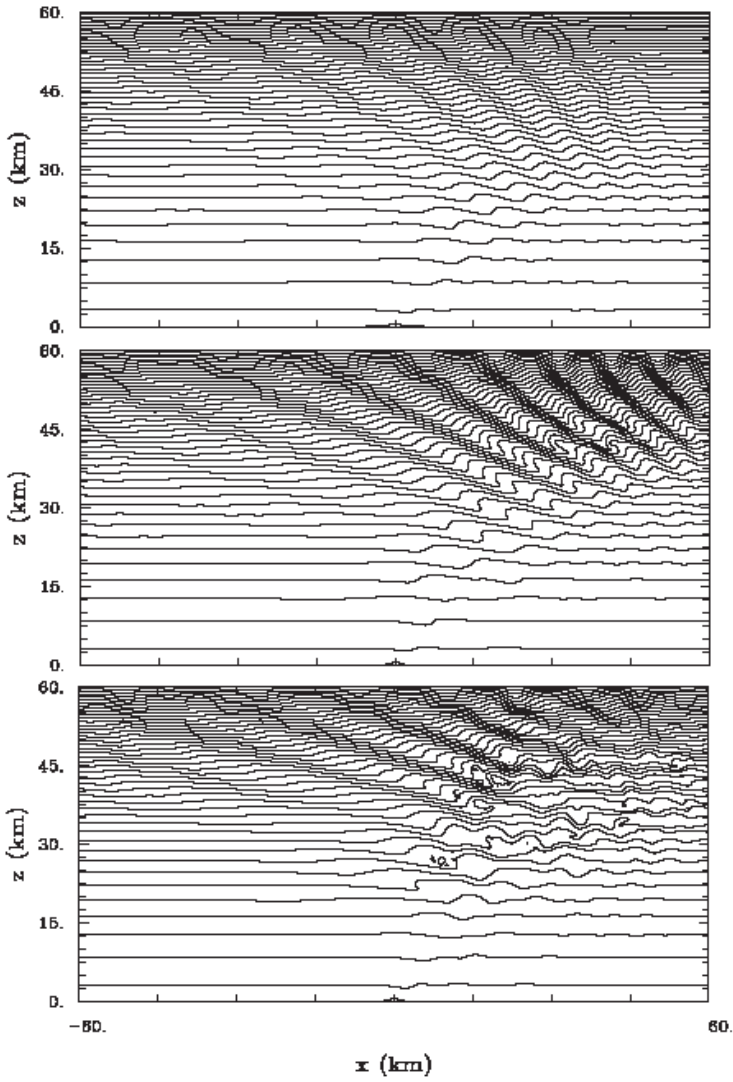

(Prusa et al JAS 1996, Smolarkiewicz & Margolin, Atmos. Ocean 1997

Klein, Ann. Rev. Fluid Dyn., 2010, Smolarkiewicz et al Acta Geoph 2011)

Smolarkiewicz et al
Acta Geoph 2011

Gravity wave breaking in an isothermal stratosphere

Nonhydristatic Edge-Based NFT

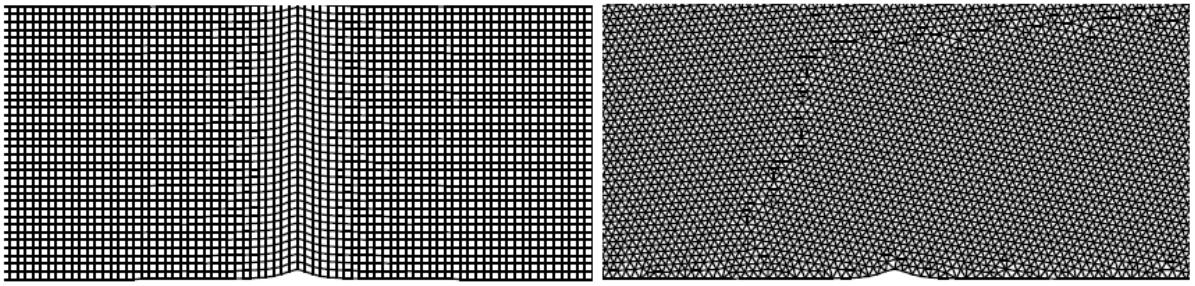

Isentropes at $t = 90$ min

EULAG *CV/GRID*

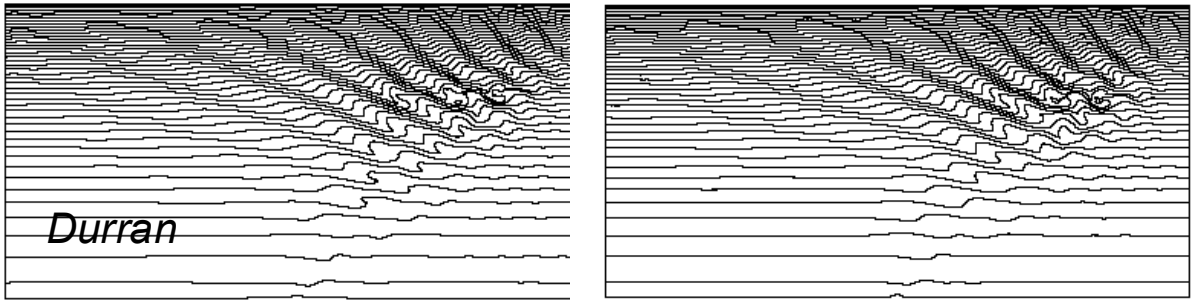

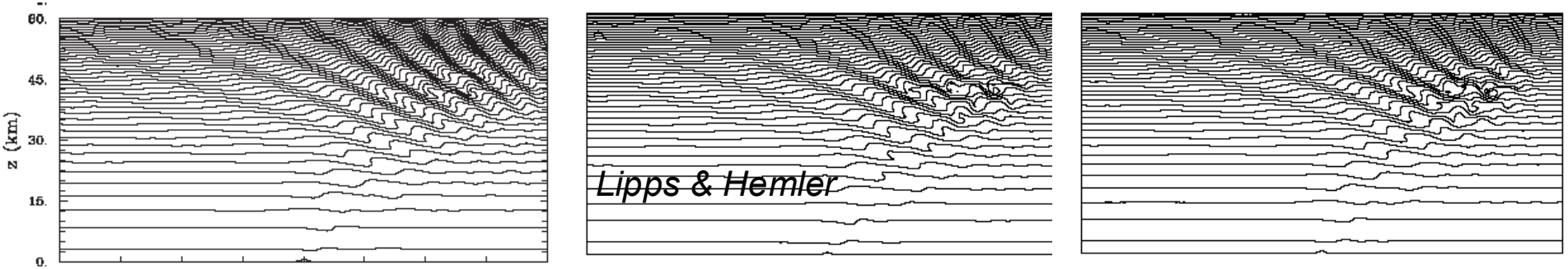

Static mesh adaptivity with MPDATA based error indicator

Schär Mon. Wea. Rev. 2002

(Recommended mesh ca10000 points)

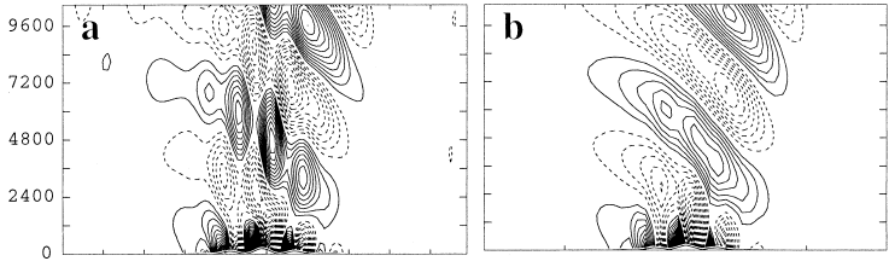

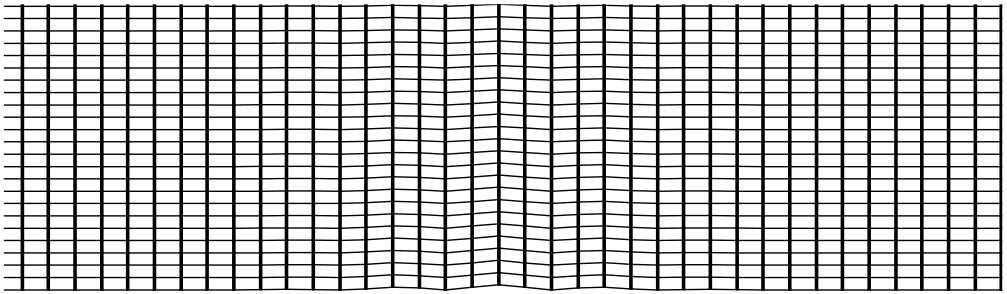

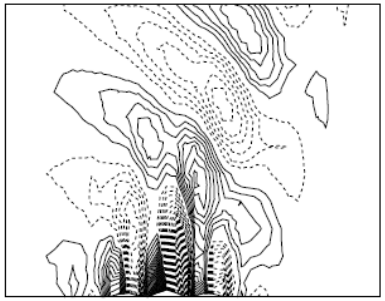

Coarse initial mesh 80x45 =3600 points and solution

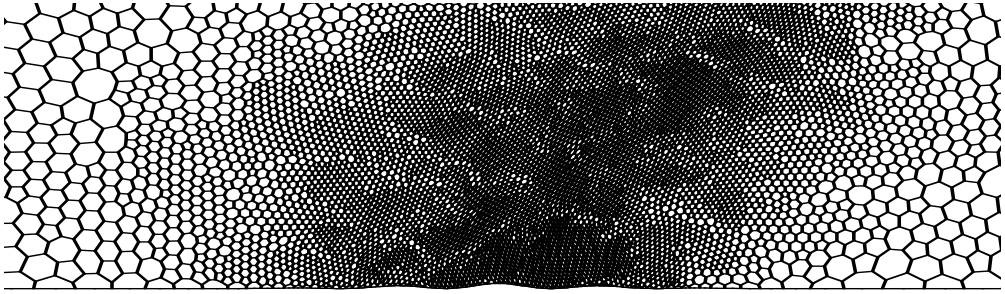

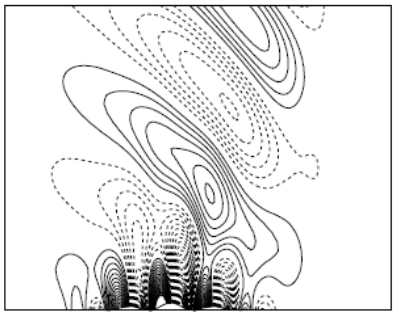

Adapted mesh 8662 points and solution

Szmelter et al JCP 2015

1121192 Cartesian dx=100
692533 Distorted prisms dx=100-400
441645 tetra dx=50 -450

Stratified flow past a steep isolated hill

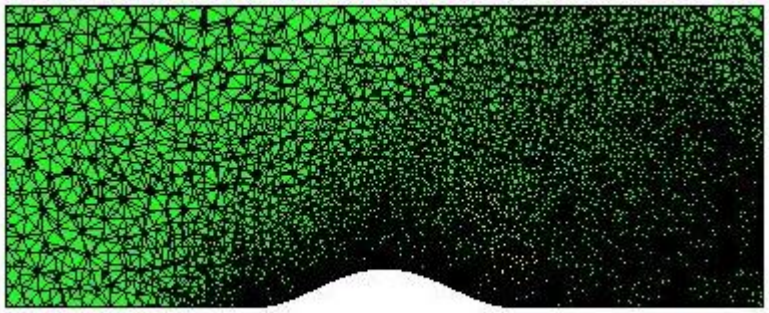

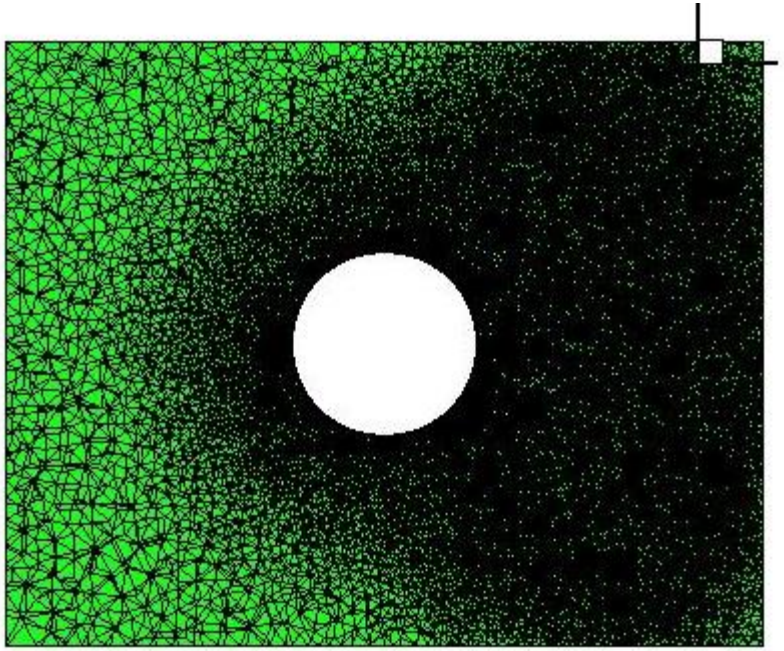

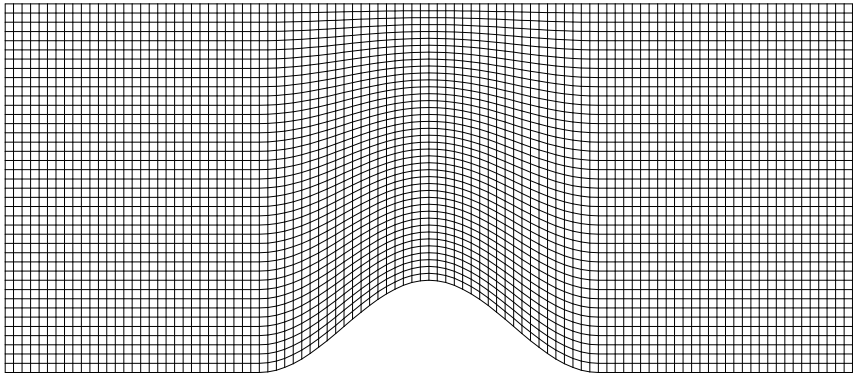

$$z_{i,k} = (k-1)\delta z \left(1 - \frac{h_i}{H}\right) + h_i \ ,$$

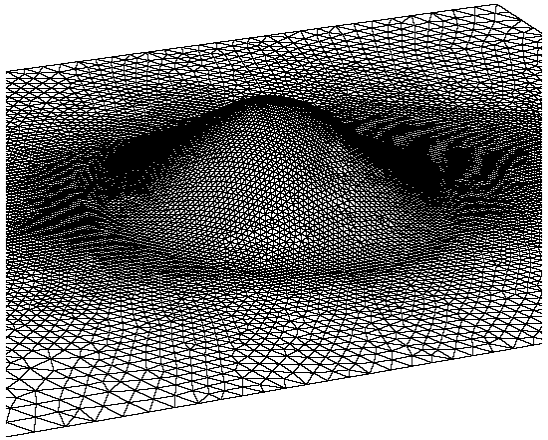

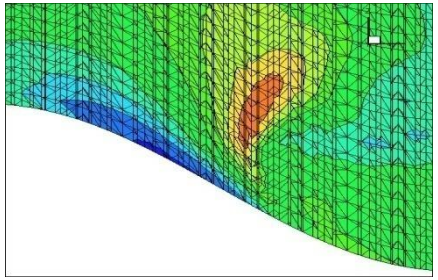

Stratified flow past a steep isolated hill

Hunt & Snyder JFM 1980
Smolarkiewicz & Rotuno JAS 1989

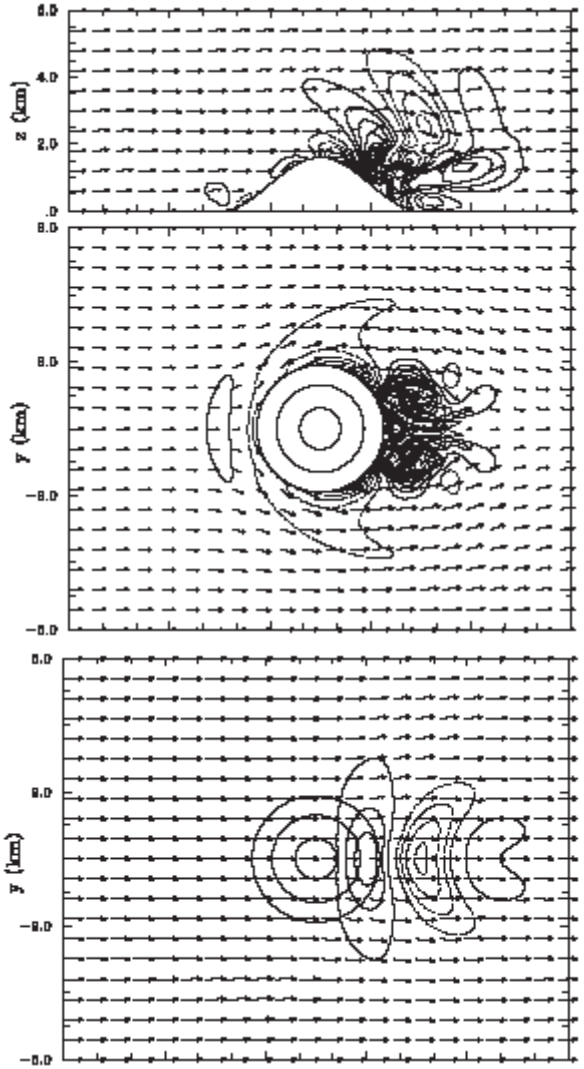

$Fr = 1/3, \ Ro \nearrow \infty$

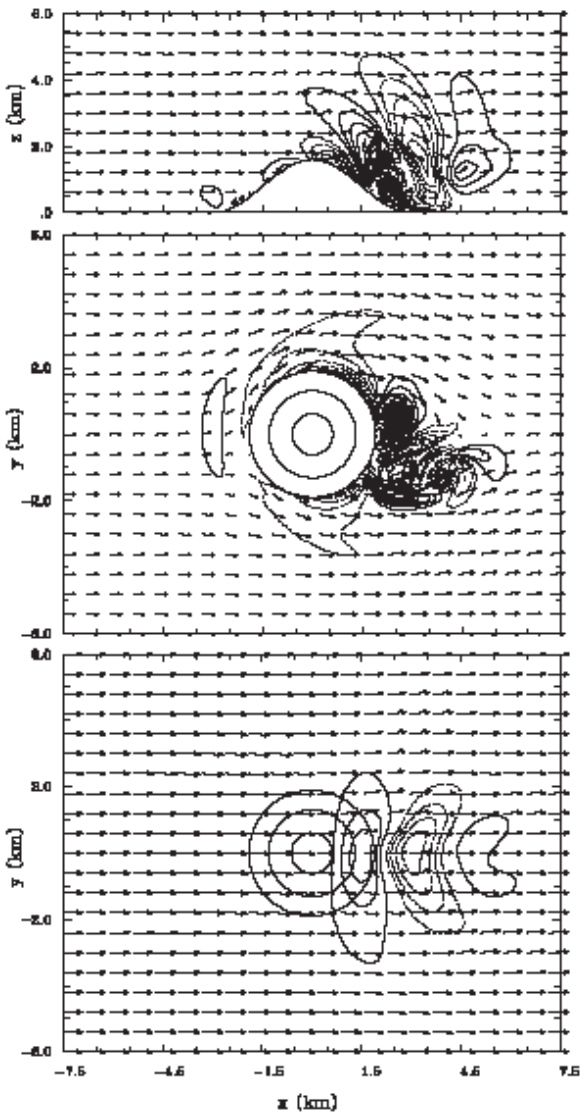

$Fr = 1/3, \ Ro \approx 3$

The effect of critical levels on stratified flows past an axisymmetric mountain

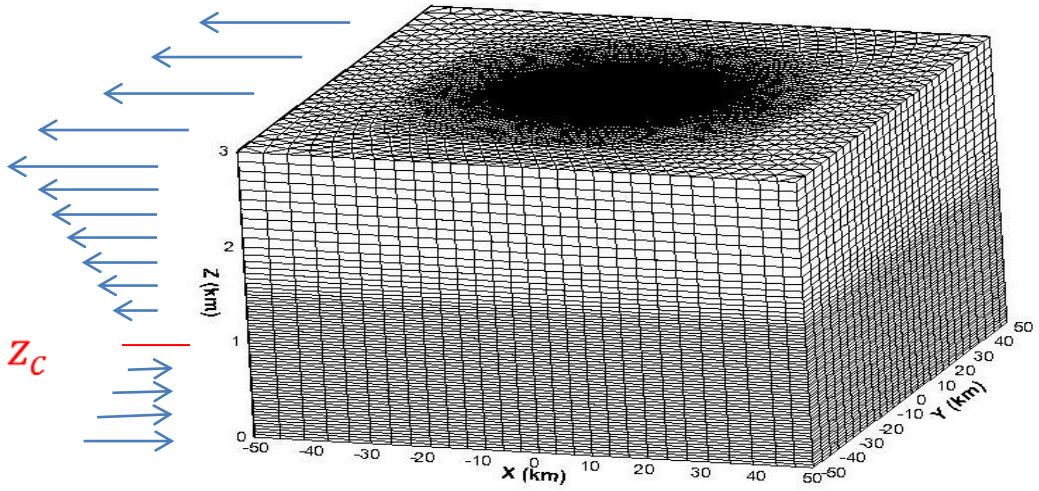

$$U_0 = 10\,ms^{-1}\,, \qquad U\,(z) = U_0\left(1 - \frac{z}{z_c}\right)$$

$$\frac{U_0}{N_a} = 0.2\,, \qquad R_i = \left(\frac{N z_c}{U_0}\right)^2 = 1\,, \qquad N = 0.01\,s^{-1}$$

$$a = 5000\,m\,, \qquad h(r) = h_0\left(1 + \frac{r^2}{a^2}\right)^{-\frac{3}{2}}\,, \qquad r \equiv \sqrt{x^2 + y^2}$$

Szmelter et. al. JCP 2015

Prismatic mesh

$$\tilde{z}_{i,k} = \tilde{z}_{i,k-1} + \delta\tilde{z}_k$$

$$\tilde{z}_{i,k} = \tilde{z}_{i,k}\left(1 - \frac{h_i}{H}\right) + h_i$$

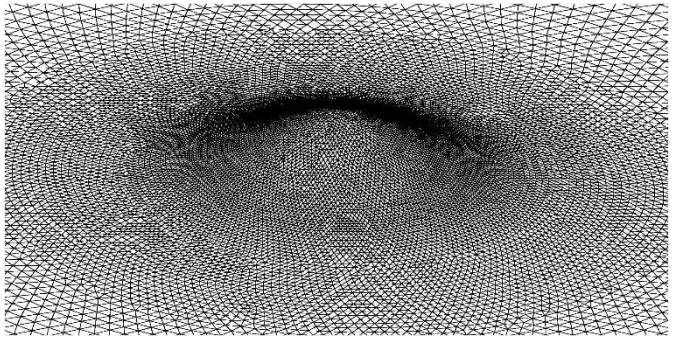

Triangular surface mesh

The effect of critical levels on stratified flows past an axisymmetric mountain

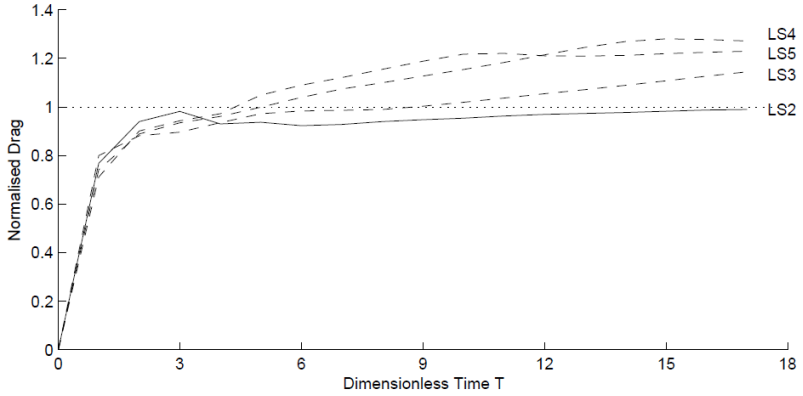

$$\hat{h} = \frac{h_0 N}{U_0} \qquad T = \frac{t U_0}{a}$$

Experiment	Ri	$\hat{h}$	$D/D_0(6)$	$D/D_0(10)$	$D/D_0(18)$
LS2 (linear)	1	0.05	0.923	0.954	0.997
LS3 (nonlinear)	1	0.1	0.983	1.02	1.160
LS4 (nonlinear)	1	0.2	1.04	1.15	1.26
LS5 (nonlinear)	1	0.3	1.09	1.22	1.23

Grubisic and Smolarkiewicz J. Atmos Sci 1997

The effect of critical levels on stratified flows past an axisymmetric mountain

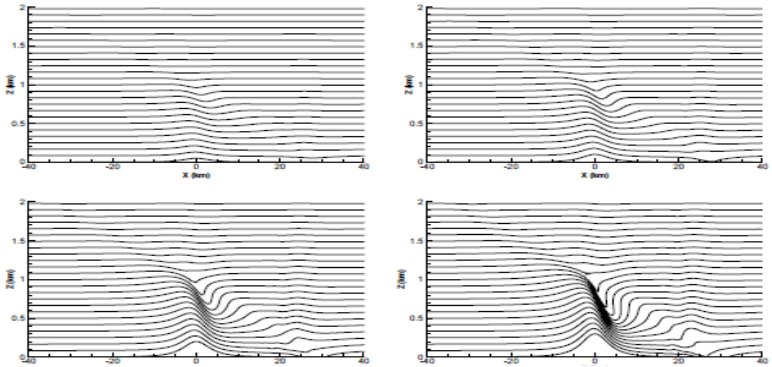

Fig. 12. Isentropes at T=6 in $y = 0$ vertical plane for experiments LS2 (left, top) LS3 (right, top), LS4 (left, bottom) and LS5 (right, bottom).

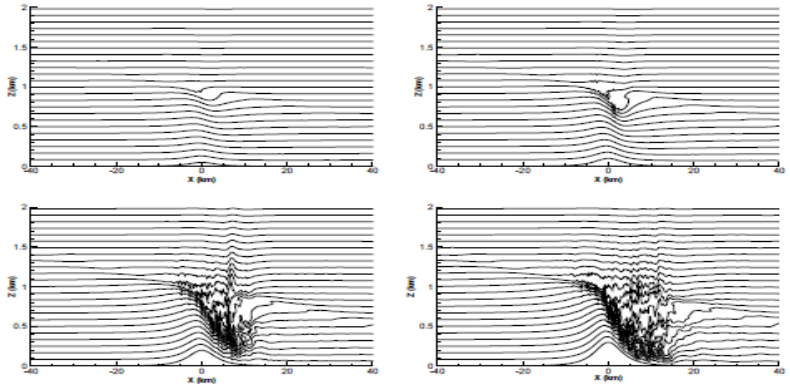

Fig. 13. As in Fig. 12 but at T=18.

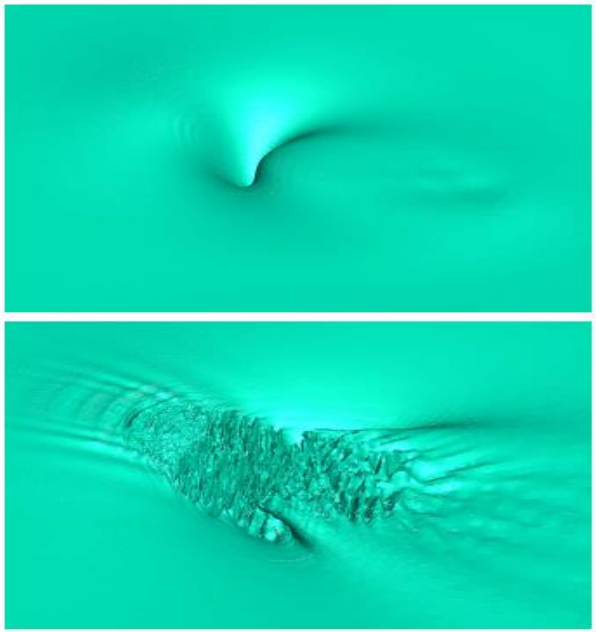

$T = 6$

$T = 18$

the isentrope with undisturbed height $z = 0.94z_c$ LS5.

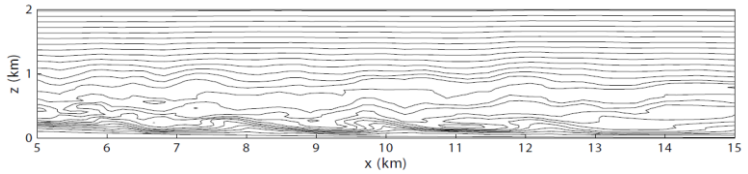

Szmelter et al JCP 2015

Stratified flow past two spheres,
Fr=0.625, Re=300

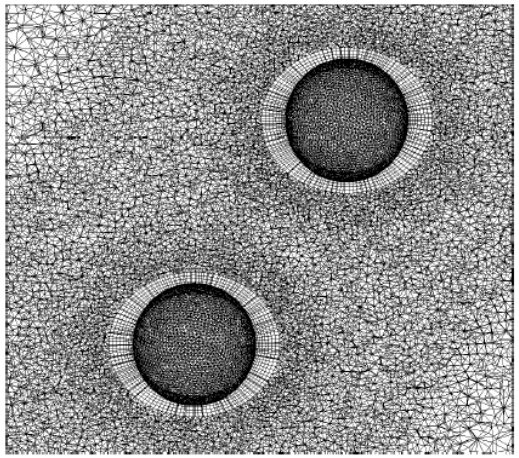

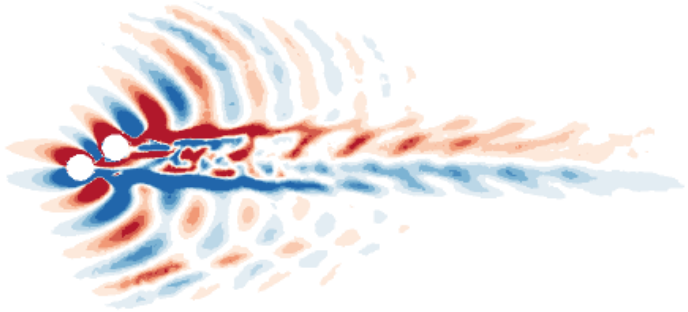

Fr=0.625
Tilted configuration

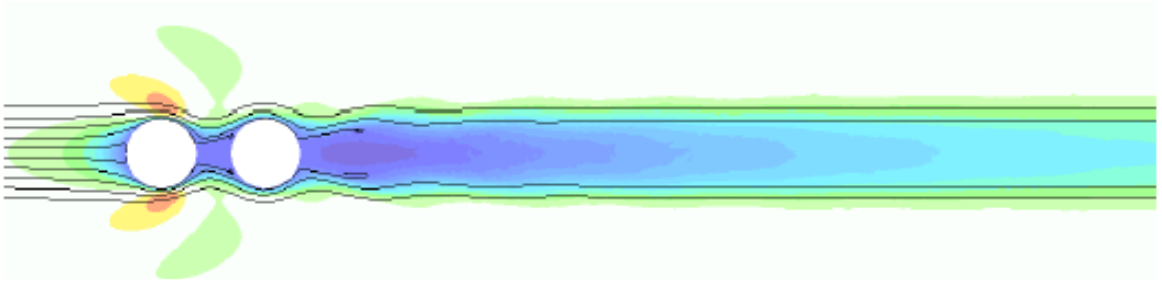

Fr=0.625

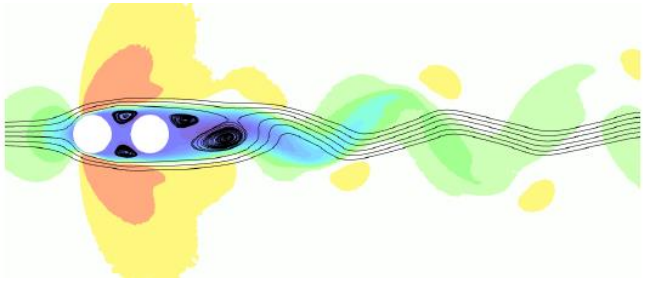

Fr=0.25

Cocetta et al PoF 2021

Convective Planetary Boundary Layer

Schmidt & Schumann JFM 1989

Smolarkiewicz et al JCP 2013

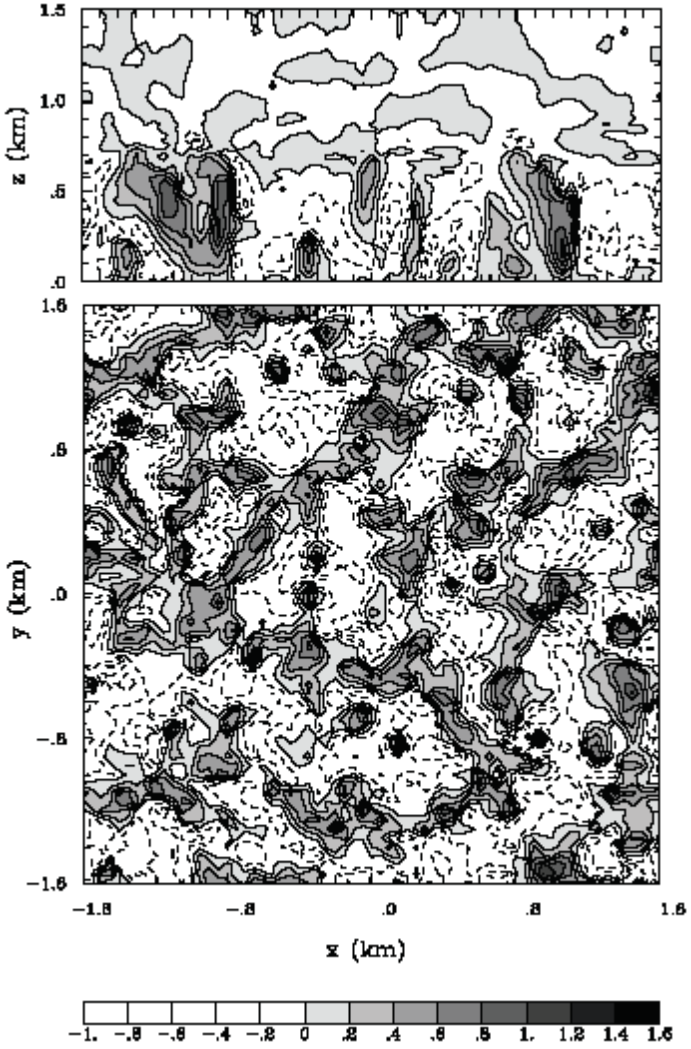

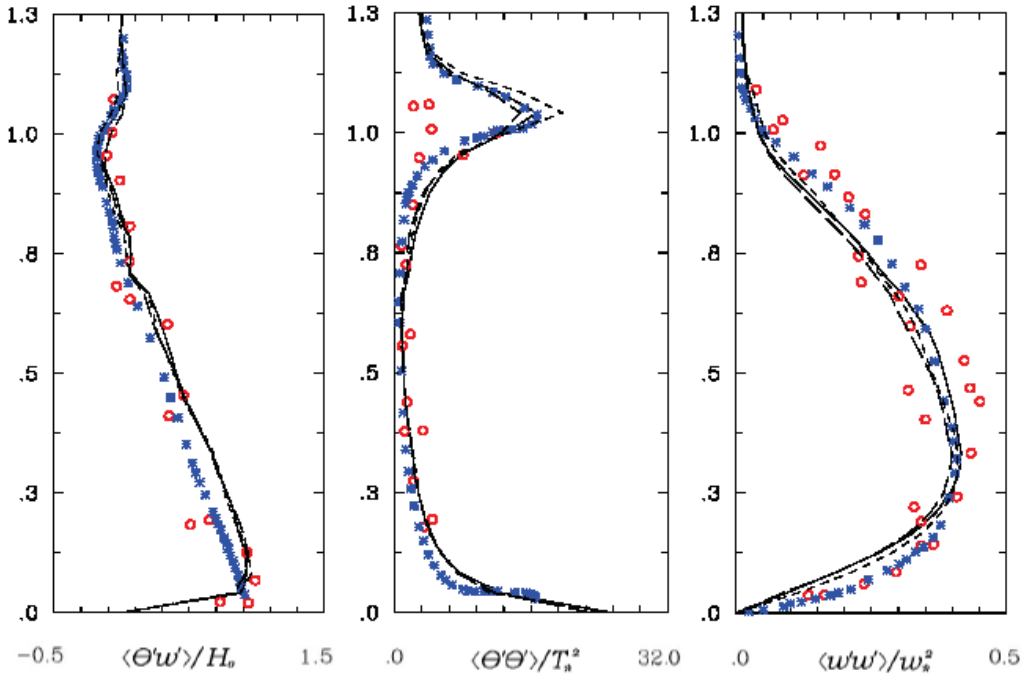

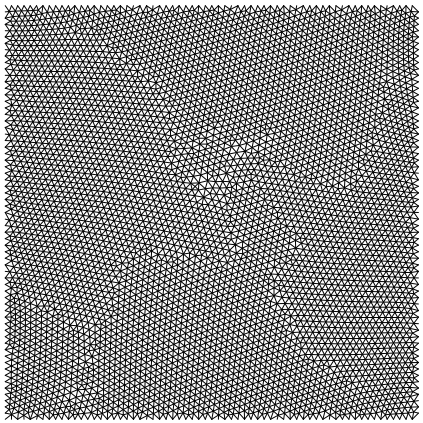

Edge-based T
Edge-based C
EULAG
SS LES
Observation
64x64x51

Selected references for further details

Cocetta F, Szmelter J, Gillard M (2021) Simulations of stably stratified flow past two spheres at Re=300, *Physics of Fluids, 334, 046602*.

Smolarkiewicz, PK, Szmelter, J, Xiao, F (2016) Simulation of all-scale atmospheric dynamics on unstructured meshes, *Journal of Computational Physics, 322,*pp.267-287

Szmelter, J, Zhang, Z, Smolarkiewicz, PK, (2015) An unstructured-mesh atmospheric model for nonhydrostatic dynamics: Towards optimal mesh resolution, *Journal of Computational Physics, 249,*pp.363-381

Smolarkiewicz, PK, Szmelter, J, Wyszogrodzki, AA (2013) An unstructured-mesh atmospheric model for nonhydrostatic dynamics, *Journal of Computational Physics, 254,*pp.184-199

Smolarkiewicz, PK and Szmelter, J (2011) A Nonhydrostatic Unstructured-Mesh Soundproof Model for Simulation of Internal Gravity Waves, *Acta Geophysica, 59(6),*pp.1109-1134

Szmelter, J and Smolarkiewicz, PK (2011) An edge-based unstructured mesh framework for atmospheric flows, *Computers and Fluids*, 46(1), pp.455-460.

Szmelter, J and Smolarkiewicz, PK (2010) An edge-based unstructured mesh discretisation in geospherical framework, *Journal of Computational Physics*, 229, pp.4980-4995.

Smolarkiewicz, PK and Szmelter, J (2009) Iterated upwind schemes for gas dynamics, *Journal of Computational Physics*, 228(1), pp.33-54

Smolarkiewicz, PK and Szmelter, J (2008) An MPDATA-based solver for compressible flows, *International Journal for Numerical Methods in Fluids*, 56(8), pp.1529-1534

Szmelter, J and Smolarkiewicz, PK (2006) MPDATA error estimator for mesh adaptivity, *International Journal for Numerical Methods in Fluids*, 50(10), pp.1269-1293

Smolarkiewicz, PK and Szmelter, J (2005) MPDATA: An Edge-Based Unstructured-Grid Formulation, *Journal of Computational Physics*, 206(2), pp.624-649

Zienkiewicz OC, Taylor RL, The Finite Element Method,5th Ed, Butterworth-Heineman, (2000)

Szmelter, J, Marchant, MJ, Evans, A, Weatherill, NP (1992) Two-dimensional Navier-Stokes Equations - Adaptivity on Structured Meshes, *Comp. Meth. Appl. Mech. Eng*, 101, pp.355-368.

Evans, A, Marchant, MJ, Szmelter, J, Weatherill, NP (1991) Adaptivity for Compressible Flow Computations Using Point Embedding on 2-D Structured Multiblock Meshes, *International Journal for Numerical Methods in Engineering*, 32, pp.896-919

Wu, J, Zhu, JZ, Szmelter, J, Zienkiewicz, OC (1990) Error Estimation and Adaptivity in Navier-Stokes Incompressible Flows, *Computational Mechanics*, 6, pp.259-270.